U.S. Department of Commerce
National Oceanic and Atmospheric Administration
National Weather Service
National Centers for Environmental Prediction
5830 University Research Court
College Park, MD 20740-3818

Office Note 514
https://doi.org/10.25923/pjs0-4j42

Current State of Data Assimilation Capabilities at NCEP's Environmental Modeling Center

Daryl Kleist, Jacob R. Carley, Andrew Collard, Emily Liu, Shun Liu, Cory R. Martin, Catherine Thomas, Russ Treadon, Guillaume Vernieres

NOAA/NWS/NCEP Environmental Modeling Center

College Park, Maryland

October 2023

Table of Contents

1 Introduction

Skill from operational numerical models continues to improve through investments in all aspects of the system. This includes increases in computing power, new observations, advanced data assimilation, and improved forecast models (Bauer et al. 2015; Simmons and Hollingsworth 2002). Data assimilation is most typically applied to obtain the best estimate of the state of the Earth system for the purposes of supplying initial conditions for a forecast. Such applications must necessarily reflect a balance between the model and observed state. This is all to ensure that forecasts are skillful and not dominated by unstable computational modes from imbalances in the initial conditions. The majority of this document will focus on the history and current status of this application of data assimilation, as it makes up a large majority of the data assimilation activities at the Environmental Modeling Center (EMC).

There is, however, a broad spectrum of applications of data assimilation within the context of Earth system modeling and prediction. Some examples of applications outside of traditional model initialization include "Analysis of Record" (AoR)[1] and reanalysis. It is useful to draw a distinction between DA methods for the production of AoR applications and those used for initial conditions in support of Earth system prediction. While both approaches use the same Bayesian principles, their underlying configurations may differ significantly. However, the restrictions imposed by balance and initialization can be relaxed for applications where the analysis is only used for situational awareness and nowcasting, verification, or calibration (i.e., AoR). There is no forecast component, allowing for a closer fit to assimilated observations. At present, the Real Time and UnRestricted Mesoscale Analysis (RTMA/URMA; De Pondeca et al. 2011) suite of systems serves this exact purpose, providing a relatively close fit to observations to serve the purposes of a gridded situational awareness system as well as for verification and ultimately calibration purposes in NOAA's National Blend of Models (Craven et al. 2020). Future advances to data assimilation algorithms must also be considered for their ability to facilitate the unique AoR application.

NCEP has been involved in several significant reanalysis efforts over the years (Kalnay et al. 1996, Kanamitsu et al. 2002, Mesinger et al. 2006, Saha et al. 2010, Hamill et al. 2021). Reanalysis efforts generally leverage the same data assimilation tools that are leveraged for the generation of initial conditions, but focus on retrospective periods with a frozen system to generate a complete, quasi-homogeneous dataset. There are generally two major drivers for the needs for reanalysis datasets: 1) climate monitoring and 2) generation of state-of-the-art initial conditions for the purposes of creating hindcasts for a particular modeling system. Reforecast datasets have been a huge advancement in the state of Earth system science, enabling exploration into aspects of the Earth systems that would otherwise not be possible.

[1]The term "Analysis Of Record" (AoR) was established in 2004 during the *Community Meeting on Real-Time and Retrospective Mesoscale Objective Analysis: An Analysis of Record Summit*. It refers to "real-time and retrospective analyses at high spatial and temporal resolution in order to facilitate the creation of the NDFD forecasts as well as verify their accuracy". Here NDFD refers to the NWS National Digital Forecast Database.

The remainder of the document is organized as follows. Section 2 provides a review and overview of the atmospheric assimilation systems with section 3 then describing the marine, land, composition, and coupled assimilation systems. Section 4 contains a comprehensive description of the use of observations in the various systems. This is followed by sections 5 and 6 that briefly describe assimilation monitoring, observation impacts, and operational implementation procedures. Section 7 then provides a brief summary.

2 Atmospheric Assimilation Systems

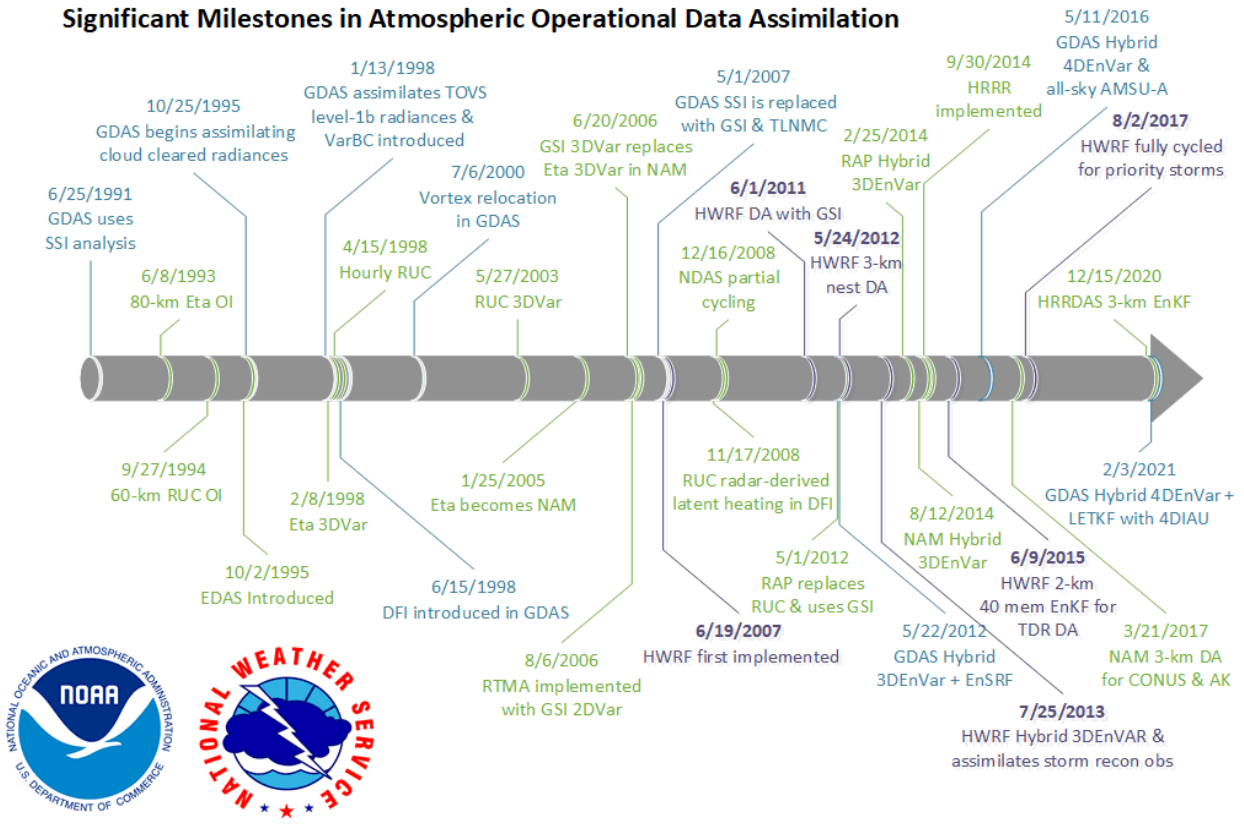

Figure 1. Timeline of significant milestones in NCEP's Operational Global and Regional Atmospheric Data Assimilation from 1991-2021.

2.1 Unification of Atmospheric Assimilation with GSI

The current NCEP Production Suite (NPS) is a complex set of disparate modeling systems to meet specific stakeholder needs. Following the recommendations of various advisory and review committees, NCEP is in the process of consolidating the production suite into a set of UFS-based applications (Unified Forecast System - Steering Committee and Writing Team 2021). For context, it is important to describe the state of the DA components that are utilized for the current NPS systems and applications. All of the atmospheric prediction and analysis systems that have assimilation components (GFS/GDAS, CDAS, NAM, RAP, HRRR, HWRF, RTMA/URMA, WDAS) currently leverage variational-based solvers.

Variational-based assimilation has been fundamental for atmospheric DA at NCEP since the first 3DVar implementation in the global model was performed with the Spectral Statistical Interpolation (SSI) analysis system (Derber et al. 1991; Parrish and Derber 1992). The ability to perform non-local analysis brought about a significant advancement in the utilization of observations by allowing for the direct assimilation of satellite radiances rather than retrievals and the use of variational bias correction (Derber and Wu 1998). Around the same time, the regional modeling system followed suit with the Eta framework which included a 3DVar implementation in the Eta Data Assimilation System in 1998 (Rogers at el. 1996).

The Gridpoint Statistical Interpolation (GSI) variational data assimilation system was originally developed (Wu et al. 2002) as a part of a major effort to provide a software framework to unify global and regional data assimilation applications. The GSI was implemented as part of the NAM/NDAS and the 2DVar RTMA (including spatially-adaptive anisotropic static covariances) in 2006 (De Pondeca et al. 2011). The GDAS/GFS followed suit in 2007 (Kleist et al. 2009a) after incorporation of the tangent linear normal mode constraint (Kleist et al. 2009b). Since then, the GSI has been deployed in the inaugural HWRF model in 2007 (Liu et al. 2006) and RAP system in 2012 (Benjamin et al. 2016). The GSI is a major accomplishment in the history of DA at NCEP; it underpins every major atmospheric prediction and analysis system in the NPS. The GSI development has clearly demonstrated the utility of having a simplified, unified framework to be leveraged across a broad swath of applications. The GSI was readily adaptable to a variety of modeling systems, and varying infrastructures, including the global spectral model, NEMS-based systems, FV3-based GFS, WRF, and more. Further, the GSI has been leveraged from other government partners, academia, and the private sector, in part through efforts to make the code available as a community code through the Developmental Testbed Center (DTC).

2.2 Hybrid Ensemble-Variational Assimilation

2.2.1 Use of ensembles

Flow-dependent, ensemble-based error covariance estimates were enabled by the development of the extended control variable method in the GSI (Wang 2010), with an initial implementation of hybrid 3DEnVar in the GDAS in 2012 (Wang et al. 2013; Kleist and Ide 2015a), which was expanded to hybrid 4DEnVar in 2016 (Kleist and Ide 2015b). The ensemble perturbations are updated using an ensemble Kalman filter (EnKF) algorithm, initially with an ensemble square root filter (EnSRF; Whitaker and Hamill 2002) and more recently with a modulated space form of the local ensemble transform Kalman filter in the GDAS (LETKF; Hunt et al. 2007; Lei et al. 2018). Importantly, the EnKF updates are GSI-based and leverage the same observation processing and operators, allowing for synergy and consistency between the perturbation update and the deterministic hybrid control analysis. Similar adaptations of ensemble-based covariances were implemented in both the NAM (Wu et al. 2017) and RAP (Hu et al. 2017) systems in 2014, first through the utilization of readily available GDAS EnKF-based members. An abbreviated timeline covering 30 years of significant milestones in atmospheric data assimilation may be found in Figure 1.

Ensemble representations of background error are now state-of-the-science and critical components of data assimilation schemes. However, ensemble forecasts have the potential to systematically underestimate the error variance due to unrepresented model errors and finite ensemble sizes, which over time can lead to filter divergence. There are many aspects of the system that can lead to errors, and there are various approaches to accounting and/or compensation for such errors (e.g. due to sampling, forward operators, model error, etc.). Covariance inflation can be performed as part of the ensemble analysis step, either on the prior or posterior covariances, and can increase the spread through an additive noise or using a multiplicative factor (Whitaker and Hamill 2012).

Multi-physics, i.e. using different physics schemes and coefficients in different ensemble members, is an effective method to increase spread in ensemble forecasts from within a model. However, it requires significant resources to not only develop but maintain many different schemes as well as to understand those schemes' interactions with other components of the physics suite. From a theoretical perspective, the ensemble error covariances derived from these members will be non-Gaussian, violating a primary assumption made in modern era data assimilation approaches. Stochastic physics parameterization is a way to increase spread through the model representation in a physically consistent way. Frequently used schemes such as Stochastically Perturbed Parameterization Tendencies (SPPT, Buizza et al. 1999) and Stochastic Kinetic Energy Backscatter (SKEB, Shutts 2005) modify the physics tendencies themselves using random pattern generators, increasing spread by representing unresolved subgrid scale processes. Additional fields to perturbed the states themselves have also proven beneficial, such as the scheme that has been used in the GDAS to perturb boundary layer humidity (Tompkins and Berner 2008). There are also recent advances toward stochastically perturbed parameters as well as building stochastic representations of the physics directly.

The current global systems, the GFS/GDAS and the Global Ensemble Forecast System (GEFS), both utilize ensemble forecasting, with short range forecasts for the GFS providing flow dependent information for the background error estimation and long range ensemble forecasts of the GEFS providing information about the model uncertainty. These two ensemble systems were initially developed independently, utilizing two separate sets of ensemble members and ensemble initialization techniques. Over time, these systems have become more aligned, first with the GEFS choosing its ensemble subset from the EnKF ensemble members (Zhou et al. 2016) and more recently with GEFSv12 (Zhou et al. 2022) adopting the same stochastic physics techniques as the GDAS (excluding the scheme that perturbs boundary layer specific humidity), though with different perturbation magnitudes and scales applied. While both applications rely on information from perturbations, spread growth in the first 6 hours of a forecast will have different characteristics than what is informative for a 30-day forecast. Recent implementations of the GEFS continue to make it more consistent with the GFS, however the implementations have not occurred concurrently, meaning that when the GFS is updated to a new resolution or new physics, the GEFS is not simultaneously updated and is no longer consistent. This discrepancy can create problems for both spread growth and balance. The planned UFS-MRW/S2S implementation hopes to bring the GFS and GEFS implementations into agreement, unifying the global data assimilation ensembles and global forecast ensembles

under one infrastructure. The goal is to have a system from which actual initial condition perturbations representative of the analysis uncertainties can be used directly in the ensemble prediction system.

The GSI-based, hybrid EnVar systems have served NCEP for well over a decade and are state-of-the-art. This document focuses on providing an overview on the current status of all data assimilation applications. It is therefore focused primarily on applications that feature the GSI. However, future plans, which are covered in detail in a companion document, involve a complete transition to a new unified data assimilation framework known as the Joint Effort for Data assimilation Integration, or JEDI. JEDI is a multi-agency effort being coordinated by the Joint Center for Satellite Data Assimilation (JCSDA) and will be the mechanism by which all of EMC's DA activities will be performed in the near future.

2.2.2 Hybrid 4D Data Assimilation

While never implemented operationally, NCEP has pursued the use of 4DVar for NWP in the past several decades. Applications of 4DVar required the development of linear versions of the dynamic model as well as its associated adjoint, to be used as part of the 4D solver. One such example was the development and utilization of a 4DVar scheme for use with the NMC Eta model (Zupanski et al. 2002a; Zupanski et al. 2002b). There were also developments at NASA's Global Modeling and Assimilation Office in the late 2000s to extend GSI to enable 4DVar for use in the GEOS system (as mentioned in Trémolet 2008), at the same time tangent-linear and adjoint versions of the GEOS system were being developed. However, computational challenges, issues associated with these developments, and competing priorities prevented them from becoming operational at NCEP.

While the implementation of traditional 4DVar was never implemented, the arrival of the hybrid EnVar era accommodated the exploration of novel innovations in the 4D framework. The incorporation of ensemble-based estimates of background error through the extended control variable in EnVar, and its natural extension to Hybrid 4DEnVar, has yielded significant improvements in the quality of analysis and subsequent forecasts. Hybrid 4DEnVar is a computationally efficient mechanism for introducing a time component to the solver without the need for linear and adjoint versions of the model within the solver. However, it is worth considering that there are a variety of hybrid assimilation algorithms that are available and have been pursued for use in numerical weather prediction. A thorough review of operational EnVar methods can be found in Bannister (2016). The primary hybrid 4D schemes are Hybrid 4DVar and Hybrid 4DEnVar. Like traditional 4DVar, hybrid 4DVar also requires the use of a linear model and associated adjoint within the solver while leveraging ensemble based representations of background error at the beginning of the assimilation window. This is in contrast with 4DEnVar which uses localized linear combinations of nonlinear forecasts throughout the window, rather than a dynamic (linear model and adjoint) model for the time evolution.

The use of Hybrid 4DVar has been shown to be superior to Hybrid 4DEnVar in a few studies that performed direct comparisons. A particularly relevant set of studies for global NWP were

performed by the United Kingdom Meteorological Office (Lorenc et al. 2015; Lorenc and Jardak 2018). In this pair of studies, it is demonstrated that while both methods are significantly superior to 3DVar and 3DEnVar, the results from trial runs show Hybrid 4DVar to be superior to Hybrid 4DEnVar. They attribute the difference to the lack of time evolution of the static component in hybrid 4DEnVar. They further demonstrate that 4DVar and 4DEnVar yield similar skill when using pure ensemble covariances. Similar findings were demonstrated with a regional modeling case study in Poterjoy and Zhang (2016). In that study, they hypothesized that the errors associated with linearization (4DVar) were less severe than errors introduced by performing four dimensional localization of the ensemble-based covariances (4DEnVar). While these studies are illustrative of the relative performance between hybrid systems with or without linear and adjoint models, they fail to (fully) take into account the computational cost associated with the relative algorithms. In addition to the need for developing and maintaining a linear model and associated adjoint to perform 4DVar, the computational cost associated with a single analysis can be an order of magnitude larger than the pure ensemble-based counterpart with reasonably sized ensembles (order 10-100).

2.3 Balance and Initialization

The need to deal with imbalances and generation of large amplitude oscillations resulting from assimilation is well documented in the literature. Within the past two decades, several mechanisms have been employed to ameliorate the impacts from such issues at NCEP. The GFS had been utilizing a full field digital filter (Huang and Lynch 1993) until the implementation of the assimilation component of GFSv15.1 (Kleist et al. 2018). One downside of such approaches is the fact that they are effectively variable independent temporal filters. In addition to undoing some of the work the analysis schemes have performed to fit the observations, they can be problematic in certain regimes. Somewhat related, latent-heat nudging has been combined with a digital filter to incorporate radar reflectivity-derived temperature tendencies as part of the RAP modeling system (Benjamin et al. 2016). A similar scheme has been utilized in the NAM data assimilation cycle (Gustafsson et al. 2018). This approach begins with a backward adiabatic filter step followed by a forward diabatic filter step where radar-derived tendencies replace those from model cloud parameterization(s). The combined effect is a balanced state with the bulk properties of observed convection represented in the initial conditions.

Within the assimilation system, the tangent-linear normal mode constraint (Kleist et al. 2009b) was developed as part of the initial implementation of the GSI to replace the SSI for use in the GFS/GDAS. This scheme has an advantage over traditional normal mode initialization techniques that had been previously employed in that it is directly integrated into the assimilation solver, effectively modifying the control variable and effective background error in the variational solver. This scheme has remained operational for global applications of GSI since the original implementation, including expansions to include the use of ensembles in EnVar. The use of the TLNMC within the context of hybrid assimilation has been demonstrated to provide significant improvements to the quality of analysis and subsequent forecast skill through improved balance (Wang et al. 2013; Kleist and Ide 2015b; Whitaker et al. 2022). This may partially be attributable to overcoming deleterious impacts induced from localization as well

as focusing on fitting observations within the space of slower modes only. While a regional version of the TLNMC within GSI was developed, it has never been utilized operationally.

Incremental analysis update (IAU, Bloom et al. 1996) is another approach that has been widely used for NWP and recently pursued by NCEP. With the implementation of GFSv16, the GDAS/GFS began utilizing 4D-IAU (Lorenc et al. 2015; Lei and Whitaker 2016). With access to 4D analysis increments from the hybrid 4DEnVar solver, hourly increments are passed to the model through the IAU forcing.

3 Marine, Land, Atmospheric Composition and Coupled Assimilation Systems

3.1 GSI-based Near Sea Surface Temperature Analysis

Unlike most NWP centers where a retrieved skin temperature field is used as the boundary condition for radiance assimilation, the sea surface temperature properties are analyzed through an additional control variable in the GSI-based atmospheric data assimilation system and are therefore more consistent with the atmospheric state. The control variable used is the "Foundation temperature", which is defined as the ocean temperature at a depth below where evaporative and radiative cooling and (solar) diurnal radiative heating from the surface are significant. These effects are modeled as part of the forward operators and are functions of wind speed and solar zenith angle.

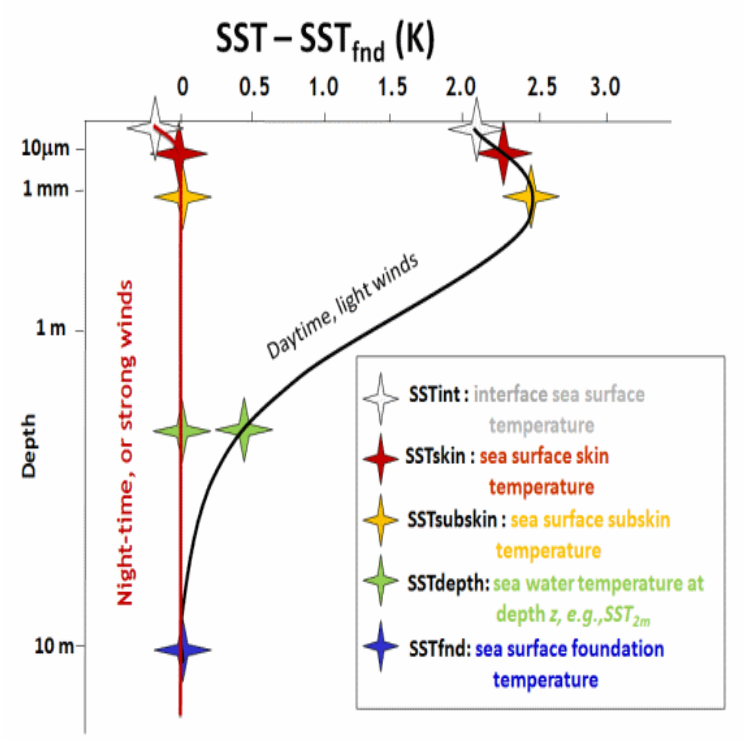

Figure 2. An illustration of the assumed profile for near sea-surface temperature. In the daytime, with light winds there is a warming in the upper 1-2m, radiative and evaporative effects result in a cooling in the upper few millimeters.

The VIIRS and AVHRR radiometers are two of the main data types used to constrain the sea surface temperature (SST) in the GSI system. While infrared radiances, due to their global coverage, are a major driver of the NSST, any observation in the GSI with a sensitivity to the sea surface temperature helps to constrain the analysis. For each observation type, a characteristic depth is assumed within the forward operator. For infrared radiances this depth is 0.015mm, for microwave it is approximately 1mm, while in situ conventional observations (ships, fixed buoys, drifting buoys, saildrones etc.) range from 0.5m - 5m. Details of the use of satellite radiances are discussed in section 5.

The inclusion of NSST as part of the operational GDAS was implemented as part of the GFS upgrade that occurred in 2017. Although the GDAS has utilized hybrid EnVar since 2012 for the atmospheric variables, the NSST-component to the GSI system was implemented using 3DVar for the foundation temperature control variable and has remained that way since the initial implementation. As the atmospheric system is not yet coupled to a dynamic ocean model, the background foundation temperature is generated by assuming persistence from one cycle to the next. The NSST-based system has gone through various upgrades in the past several years to incorporate new datasets and calibrate background/observation errors. It has since begun providing boundary conditions for downstream models, replacing previously used products such as Reynolds/OI and RTG-SST. See Figure 2 for an illustration of the assumed profile for NSST in the GDAS.

3.2 Component assimilation systems

The current operational version of the Global Ocean Data Assimilation System (GODAS) originated from the global 3DVar system developed at the Geophysical Fluid Dynamics Laboratory (GFDL) (Derber and Rosati 1989, Behringer et al. 1998, Behringer 2007). The GODAS system was developed around MOM-based ocean modeling for use in climate monitoring and seasonal prediction, and was included as a component of CFSv1 (Saha et al. 2006). The more recent CFSv2/CFSR/CDAS (Saha et al. 2010) included the use of MOMv4 and weakly coupled assimilation, with the atmospheric component being driven by a GSI-based 3DVar system. Separately, the operational ocean prediction system, RTOFS, is currently a HYCOM-based modeling application with initialization coming from the US Navy Coupled Ocean Data Assimilation (NCODA) system. In 2013, EMC signed an Memorandum of Understanding (MOU) with the Naval Research Lab to port NCODA to NWS supercomputers, allowing for access to internally produced initial conditions rather than relying on an external data feed. The NCODA based 3DVar assimilation system was implemented as RTOFS-DA as part of RTOFSv2. Plans are already underway for unification of the assimilation systems to be MOM- and JEDI-based. An initial effort has recently been completed under the auspices of the UFS-R2O project to complete a 40 year marine reanalysis (MOM6/CICE6 + JEDI-3DVar), the so-called interim Next-Generation GODAS (ng-godas) project, demonstrating the maturity and efficacy of such a path forward for future UFS-based applications (Kim et al. 2022).

Land data assimilation has evolved to be a mix of directly inserted products and observationally forced land model integration. The North American Land Data Assimilation System (NLDAS)

and Global Land Data Assimilation System (GLDAS) are based on the Noah land surface model, leveraging the offline NASA/Land Information System (LIS) as a driver and means of integrating observed quantities such as precipitation to update soil moisture. The NLDAS has been leveraged for initialization of regional land components and North American drought monitoring, whereas the GLDAS was included as part of the CFSR/CFSv2 and GFSv16. At present, the RAP and HRRR are the only operational systems that employ a so-called moderately coupled land-snow-atmosphere assimilation approach (Benjamin et al. 2022). This method is a one-way coupling via a simple covariance model between the near-surface atmospheric analysis increment and underlying soil-snow state. Work is now underway to develop JEDI-based land assimilation capabilities, including state estimation of quantities like snow and soil moisture, for use in the future UFS-coupled applications that will leverage Noah-MP (and/or other updated land models).

While many NWP centers currently perform operational analyses of global aerosol species, atmospheric composition DA in the NWS is still in its infancy. The GEFS-Aerosol component, in operations since fall 2020, incorporates fire emissions derived from satellite observations, but no direct assimilation of retrievals or radiances is performed in this system, the aerosol tracer values are merely carried between forecast cycles. Looking ahead, a coordinated effort is now underway between NWS and NOAA OAR labs to develop an initial capability to use JEDI to assimilate aerosol optical depth (AOD) retrievals into a global aerosol prediction system. While the focus of the existing composition DA work has been on global aerosols to support improved subseasonal to seasonal (S2S) prediction capabilities, there is a parallel effort towards improving the NWS's regional air quality forecasting system. Less mature than the global AOD effort, work funded by Disaster Relief Appropriations is underway on the initial exploration of assimilation of AOD as well as nitrogen dioxide (NO_2) retrievals and surface in-situ particulate matter ($PM_{2.5}$) observations into an online coupled regional air quality prediction system as part of RRFS.

4 Current Use of Observations

Observations are a foundational component to all aspects of environmental modeling and prediction, especially DA. Our current data assimilation systems are mature and assimilate a variety of observations from a diverse range of instruments (Tables 1-15). Such observations include relatively standard platforms like rawinsondes, dropsondes, buoys, METAR, satellite radiances, and bending angles from Global Navigation Satellite System-Radio Occultation (GNSS-RO). However our systems also routinely use more unique datasets, such as NOAA P-3 provided Doppler radar winds from intense tropical cyclones, crowd-sourced personal weather station observations, and synthetic observations derived from official tropical cyclone advisory centers. This section will summarize the current use of observation in operational data assimilation for each data type.

4.1 Decoding and Observation Processing

Environmental observations arrive for operational assimilation from many sources and mechanisms and in a variety of formats. Decoding, reformatting, and preprocessing the

observations are critical for successful assimilation. The existing set of codes that performs these tasks were developed over several decades. The current workflow involves the receipt of data from a variety of sources, where observations are ingested, gathered, and decoded into standard Binary Universal Form for the Representation of meteorological data (BUFR) files. These files are then run through utilities to create a database of continuously populated NCEP BUFR tanks. The tanks are then converted into BUFR dump files for various applications. The dump step includes temporal and geographic filtering, duplication-checking, and preliminary quality control (QC) of data depending on the application. The quality control done at this step is pre-screening in nature and generally based on known purge flags and reject lists. For some observation types, dump files are read in directly by the application, such as the assimilation or verification codes. However, additional processing and quality control occur to create the NCEP prepBUFR file for selected in situ observations. A schematic representation of the workflow involved is presented in Figure 3.

Like other aspects of the system, the preprocessing software requires reengineering, modernization, and generalization for the future. Technical difficulties are already being incurred in the transition to full integration of BUFR-disseminated observations, new and updated formats, large volumes of new data, and other unanticipated changes in aspects of the global observing system. JEDI-based infrastructure is envisioned to be a focal point for an overhaul of many aspects of the preprocessing software. A project to scope out the use of JEDI-based tools to replace legacy preprocessing infrastructure is underway and discussed as part of the 10-year strategy for DA (Kleist et al. 2023). However, work has already begun in earnest to enable the use of observations in current and future JEDI-based systems by working toward refactoring legacy observation processing and ingest codes (see Appendix).

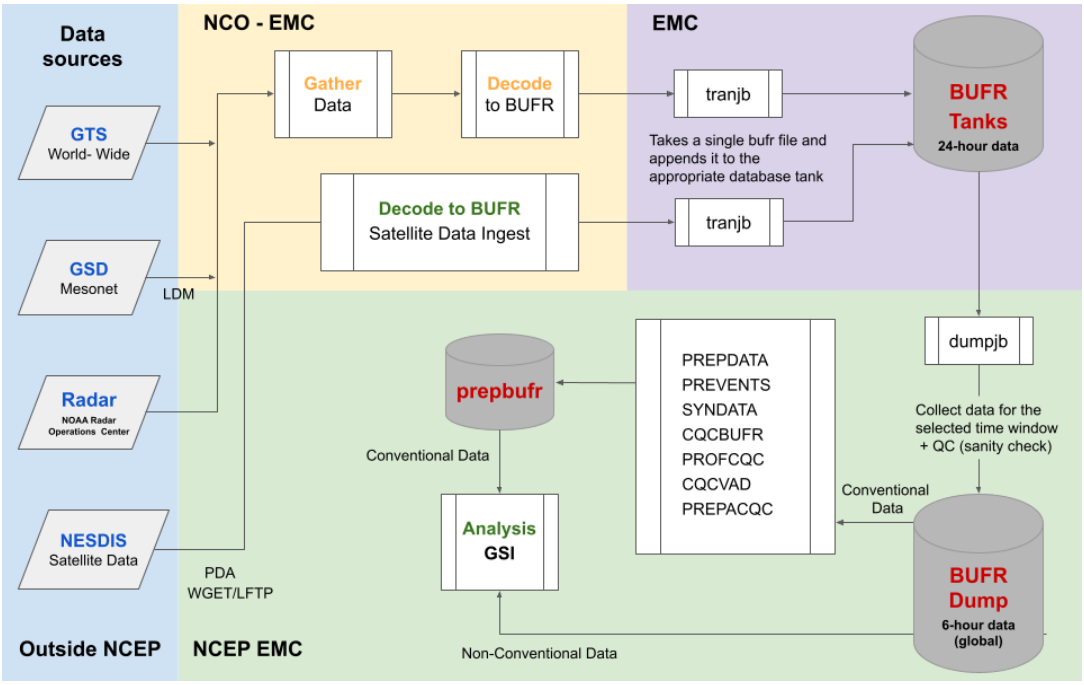

Figure 3. Schematic representation of the operational ingest, decoding, and observation preprocessing process.

4.2 In-situ and anchor observations

NCEP currently assimilates a variety of in situ observations such as radiosonde, aircraft, buoy, surface station, dropsonde, and many more (Example distribution in Figure 4), to constrain temperature, moisture, wind, surface pressure, and sea surface temperature analysis. These observations along with GNSS-RO data serve as anchor data to prevent analysis drift. The utilization of the in situ data has been enhanced with variational quality control (VarQC; Purser 2018b). It is not a criterion for rejection; rather, it is a re-weighting of observations. With VarQC, it is possible to significantly loosen the gross check and accept outliers into the assimilation. Hence, every observation can contribute to the analysis, but those with large departures between the observed and the simulated measurement will be strongly down-weighted. This is achieved by reformulating the observation cost function such that the probability distribution function conforms to a predetermined shape, for example a Huber norm distribution which is currently used in our operational systems. The predetermined shape generally exhibits tails broader than those of the familiar Gaussian (e.g. the source of the downweighting of deviant observation that Bayesian theory implies).

4.2.1 Surface observations

A wide variety of surface observations are routinely assimilated everyday in NCEP's operational prediction systems. These include land and sea-based platforms, university-sponsored mesonets, and even crowd-sourced observations from citizen scientists. These are currently largely only used in the regional modeling systems and analysis of record (e.g. Morris et al. 2020), with a subset feeding directly into the GFS/GDAS.

Over land, we assimilate observations from standard aviation routine weather report (METAR) platform[2]. In the global system, this is limited to surface pressure, but for regional applications other quantities are assimilated, including 2 m AGL temperature and moisture, 10 m AGL wind along with ceilometer observations of cloud ceiling sky cover as well as visibility. The latter cloud ceiling and visibility fields are especially important in aviation applications, and are either directly assimilated via control variable transformation (e.g. Yang et al. 2020) or diagnosed through cloud analysis techniques (Benjamin et al. 2021). Similar observations are also assimilated from university-sponsored networks, road weather information systems, remote automatic weather stations, as well as those provided from programs like the Citizen Weather Observers Program (CWOP). The latter represents a large, crowd-sourced data set of observations provided from the general public. Each network possesses unique error characteristics, and in the case of networks with limited to absent instrument and siting standards (crowd sourced), strict quality measures are enforced. Further, recent advances of renewable energy projects have led to the emergence of meteorological tall tower observations and anemometers mounted atop turbine nacelles, the latter of which have been used in experiments but not yet in operations (Wilczak et al. 2015).

[2] E.g., Automated Surface Observing System, Automated Weather Observing System and SYNOP

Surface-based marine observations are routinely assimilated and come from platforms such as moored and drifting buoys, the Coastal-Marine Automated Network (C-MAN), fixed (including tropical moored buoy arrays such as TAO) and drifting buoys, ships, gliders, Saildrones, and a fraction of Argo floats sampling the near surface. Observations include near-surface variables of temperature, moisture, and wind alongside observations of wave height, sea surface or near surface temperature, salinity and surface current.

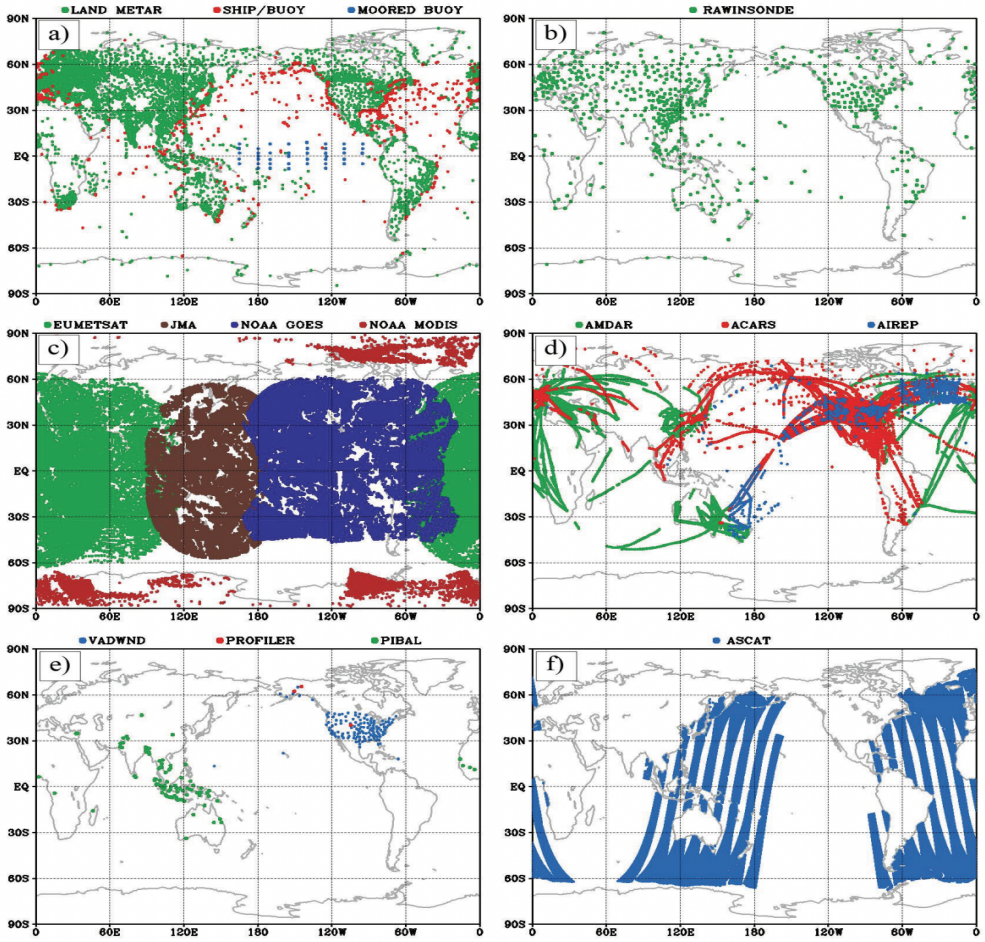

Figure 4. Spatial distribution for atmospheric observations for the 6-hour window centered at 00 UTC on April 15, 2015, including (a) surface, (b) rawinsonde, (c) atmospheric motion vectors (AMVs), (d) aircraft, (e) Velocity Azimuth Display (VAD) winds, lidar wind profilers, and pibal balloons, and (f), and Advanced Scatterometer (ASCAT) derived surface wind speeds. Figure 5.2 from "Next Generation Earth System Prediction: Strategies for Subseasonal to Seasonal Forecasts (2016)", DOI 10.17226/21873.

BUFR Type 000 Surface Data Land				
Subtype	**Mnemonic**	**Description**	**Original Format**	**Restricted**
000 100	synopr	Synoptic report from fixed land station manual & automatic	WMO BUFR	Yes
001 101	synop	Synoptic report from fixed land station manual & automatic	WMO BUFR	No
002 102	synopm synopmb	Synoptic report from a mobile land station manual & automatic	WMO BUFR	No
007	metar	Aerodrome routine meteorological report - METAR Aerodrome special meteorological report - SPECI	WMO	No
010	shefcm	Product from SHEF format	SHEF	No
011	sheff	Automation of Field Operations and Services (AFOS), mainly precipitation	SHEF	No
015	N/A	Snow reports: snow cover, depth/density and water equivalent	BUFR	No
020	nacell	Meteorological data collected from NACELLE (wind turbine)	netCDF	Yes

Table 1. EMC operational data inventory for surface land data.

4.2.3 Marine Observations

The sub-surface in situ observing system consists of eXpendable Bathythermographs (XBTs), Conductivity Temperature Depth (CTD) sensors, tropical moored buoy arrays (TAO/TRITON, RAMA and PIRATA) for the observation of subsurface temperature, salinity, currents and biogeochemistry variables. Subsurface data from the Argo platform is also used for initializing marine applications including RTOFS. ARGO subsurface data is critical for operational RTOFS because of a general lack of any subsurface observations over large regions. Underwater gliders are also ingested at NCEP and are currently the the only source of high resolution in situ measurement able to resolve the ocean at the sub-mesoscales.

BUFR Type 001 Surface Data Sea				
Subtype	Mnemonic	Description	Original Format	Restricted
001 101	ships	Ship - manual & automatic	WMO BUFR	Yes
013 113	shipsu	Ship - manual & automatic	WMO BUFR	No
002 011 102	dbuoy buoysh dbuoyb	Drifting Buoy	WMO SHEF BUFR	No
003 011 103	mbuoy buoysh mbuoyb	Moored Buoy	WMO SHEF BUFR	No
004 010 104	lcman cmansh lcmanb	Coastal-Marine Automated Network (C-MAN)	CMAN SHEF BUFR	No
005 008 012	tideg tidgcm tidgsh	Tide Gauge	CREX CMAN SHEF	No
007	cstgd	U.S. Coast Guard reports	Local ASCII	No
009	river	USGS River/Stream data	Local ASCII	No
014		River Forecast (RVF) data	SHEF	Yes
021		Canadian Water Level	Local ASCII	No
022		Canadian Water Gauge	Local ASCII	No
120		Saildrone (uncrewed surface vehicles)	BUFR	No

Table 2. EMC operational data inventory for surface marine data.

4.2.4 Rawinsondes

One of the most important in-situ observing systems for NWP is the global rawinsonde network. Rawinsondes are launched from the ground and carry an instrument package through the troposphere, providing vertical profiles of temperature, moisture, pressure and winds. Rawinsonde launches are a coordinated, worldwide effort that generally occur twice a day, everyday, producing profiles valid at 00 UTC and 12 UTC. Additional launches may occur at

times besides those mentioned if there is a situation that warrants more in-situ observations in the troposphere such as before anticipated severe weather outbreaks. While higher resolution (vertical and temporal) radiosonde information is now becoming available through direct transmission and dissemination directly in BUFR, the current infrastructure is largely reliant on the older Traditional Alphanumeric Form (TAC) disseminated information with a few exceptions. This is discussed in more detail in the 10-year strategy (Kleist et al. 2023).

BUFR Type 0002 Vertical Soundings Upper air and Dropsondes				
Subtype	**Mnemonic**	**Description**	**Original Format**	**Restricted**
001 101	raobf	Rawinsonde from fixed land station	WMO BUFR	No
002 102	raobm	Rawinsonde from mobile land station	WMO BUFR	No
003 103	raobs	Rawinsonde from ship	WMO BUFR	No
004 104	dropw	Dropwindsonde	WMO BUFR	No
005 105	pibal	Pilot Balloon (PIBAL) wind observations from land, ship, and mobile stations	WMO BUFR	No
020	towerr	Wind Energy Tower (future)	netCDF	Yes
021	towern	Wind Energy Tower (future)	netCDF	No

Table 3. EMC operational data inventory for vertical soundings: upper air and dropsondes.

4.2.5 Reconnaissance-based

4.2.5.1 Dropsondes

Similar to rawinsondes, dropsondes provide tropospheric profiles of temperature, moisture, pressure, and wind but are released from aircraft, often as a part of a field reconnaissance mission. Observations are taken as the dropsonde descends toward the surface. The data are transmitted during descent and received at NCEP for assimilation. Dropsondes are deployed in a variety of weather regimes, and are most commonly employed over the ocean where positioning for a rawinsonde release by ship is inconvenient. Dropsondes are typically employed as a part of tropical storm reconnaissance efforts, but have been employed for rapidly developing mid-latitude cyclones, and to provide in-situ observations of atmospheric rivers (e.g. Wilson et al. 2021). These types of observations have been shown to provide a positive impact on GFS forecasts for tropical cyclones (Brennan et al. 2015) and atmospheric rivers (Lord et al. 2023).

4.2.5.2 Aircraft mounted radar

A special case of Doppler radar data comes from the NOAA P3 aircraft, which are outfitted with X-band radars on the tail portion of the aircraft, called tail Doppler radar (e.g., Jorgensen et al. 1983). These radars collect observations of tropical cyclones (Gamache et al. 1995) and transmit the radial velocity data to NCEP for assimilation. NCEP has been receiving these observations since 2010, and they are used in the regional hurricane applications (e.g., Tong et al. 2018).

4.2.5.3 Flight level aircraft reconnaissance data

Reconnaissance aircraft are typically outfitted with instrumentation so that they may measure flight-level winds, temperature, and moisture. This data is then transmitted from the aircraft via the high-density observations bulletin (HDOB) directly to NCEP for assimilation. Such observations typically accompany reconnaissance missions involving NOAA P-3 and other research aircraft. In addition to flight-level observations, HDOB can also include near surface wind speed measurements from the Stepped Frequency Microwave Radiometer mounted on the reconnaissance aircraft. When available, these observations are used in operations in hurricane applications. For the GFS/GDAS, HDOB observations are assimilated via dump files (e.g. not via prepBUFR).

BUFR Type 004 Single Level Upper-Air Data Reconnaissance			
Subtype	**Mnemonic**	**Description**	**Restricted**
005	recco	Flight level reconnaissance aircraft data	No
015	hdob	High density aircraft observations (HDOB) from reconnaissance aircraft data	No
070	tldplr	P3 Aircraft Tail Doppler radar (TDR) radial wind	No

Table 4. EMC operational data inventory for reconnaissance aircraft data, including radial wind.

4.2.6 Aircraft

Aircraft observations are a major source of information in the NWP systems with significant geographic coverage (Figure 5). They provide in-situ flight level and, around airports, profile information on temperature, humidity, and wind fields. Data are provided through a number of sources: the Aircraft Meteorological DAta Relay (AMDAR) which was initiated by the WMO to relay existing measurements from aviation partners; Meteorological Data Collection and Reporting System (MDCRS) which is a similar system run by NOAA; and Tropospheric Airborne Meteorological Data Reporting (TAMDAR) which is a bespoke weather monitoring system run by FLYHT Aerospace Solutions.

There are two main challenges with the use of aircraft observations. The first is that the aircraft observations are often biased with respect to nearby radiosonde measurements and the second

is that the large density of observations around airports (and elsewhere if the reporting frequency is high enough) can result in the analysis drawing too closely to the measurements (representativeness errors becoming the dominant term).

Aircraft biases are corrected in the analysis with a variational bias correction scheme (Zhu et al., 2015). Currently this is limited to temperature observations. The scheme uses three predictors: a constant term, the aircraft vertical velocity and the square of the vertical velocity. Coefficients for each of these predictors are assigned for each individual aircraft (based on tail number). A novel approach based on projecting the observations onto a Hilbert curve has been developed to address the issue of excessive clustering of observations (Purser 2018a). This is an efficient way to increase the observation error in high observation density areas, thereby down-weighting the impact without completely removing otherwise good data. This is currently applied in the operational GFS for wind observations only.

An interesting opportunity to observe the impact of a loss of a significant amount of commercial aircraft data associated with travel restrictions and lockdowns in 2020 during the early stages of the COVID-19 pandemic. While it is well documented that aircraft-based observations do improve the quality of analysis and subsequent forecast, particularly for certain applications such as the Rapid Refresh model (James and Benjamin 2017) and for individual metrics like upper tropospheric winds, no obvious loss of skill was observed by international partners during the early days of the pandemic (Ingleby et al. 2021). This is one demonstration of the robustness of certain aspects of the global observing system, particularly for modern day numerical weather prediction.

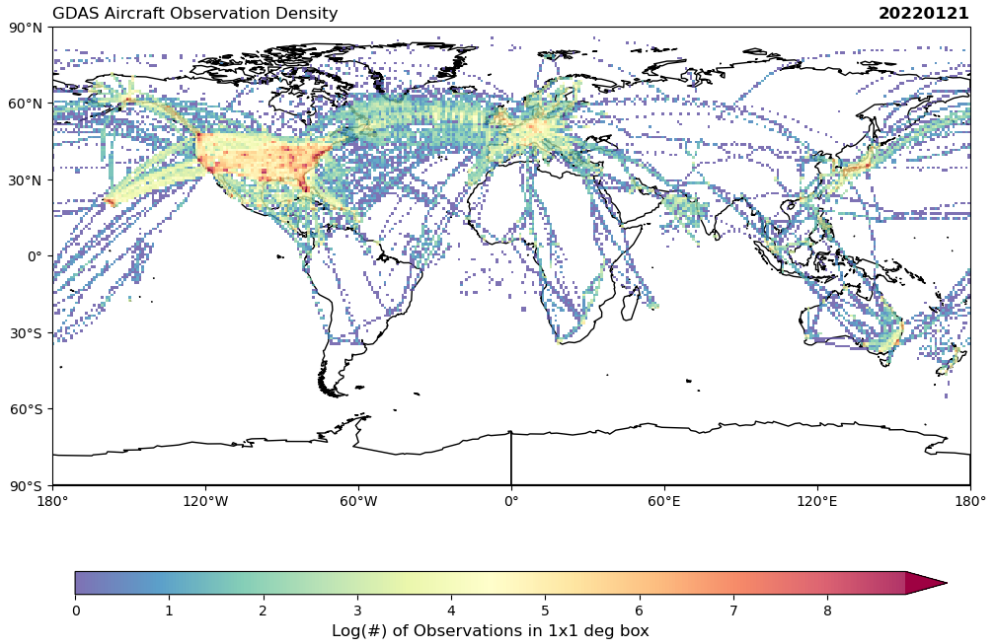

Figure 5. Log(number of aircraft observations in a 1° box) for all four GDAS cycles on January 21, 2022.

BUFR Type 004 Single Level Upper-Air Data Aircraft			
Subtype	**Mnemonic**	**Description**	**Restricted**
001	airep	Manual AIREP (Aircraft Report) format data Automated Automatic Dependent Surveillance (ADS) aircraft	No
002	pirep	Manual PIREP (Pilot Report) format aircraft data	No
003	amdar	Automated AMDAR (Aircraft Meteorological Data Relay) system aircraft data	Yes
004	acars	Automated MDCRS system aircraft data from ACARS managed by ARINC MDCRS = Meteorological Data Collection and Reporting ACARS = Aircraft Communications Addressing and Reporting System Aeronautical Radio, Inc. = ARINC	Yes
006	eadas	European automated AMDAR aircraft (E-AMDAR) data	Yes
009	camdar	Canadian automated AMDAR aircraft data	Yes
010	tmdara	Automated TMDAR (Tropospheric Meteorological Data Relay) system data from Panasonic	Yes
011	kamdar	Korean automated AMDAR aircraft data	Yes
103	amdarb	Automated AMDAR aircraft data	Yes

Table 5. EMC operational data inventory for single-level upper air data (aircraft).

4.3 Remotely sensed (non-satellite)

4.3.1 Profiler (and LIDAR, vertically pointing radar etc.)

Upward facing atmospheric profilers can provide different information depending on the design of the instrument and the wavelengths used. For example, fixed Doppler radars can provide vertical profiles of atmospheric winds and combined with a Radio Acoustic Sounding System (RASS), can also provide virtual temperature profiles. Depending on the size and type of the profiler, these observations can be limited to just the planetary boundary layer, or can stretch to as high as the lower stratosphere. In the visible spectrum, LIDAR can give information on lower-level moisture, temperature, aerosols, and derive the height of the boundary layer.

4.3.2 Doppler Radar

The NWS operates a network of S-band Doppler dual polarization weather radars across the U.S. and territories. This network constitutes the only observing system capable of providing high resolution spatiotemporal observations of deep convective storms, making it an especially valuable data set for convective-scale data assimilation. Both Doppler radial velocity and reflectivity are assimilated in NOAA's regional systems.

BUFR Type 002 Vertical Soundings Profilers			
Subtype	**Mnemonic**	**Description**	**Restricted**
009	prflrp	Profiler winds originating from PIBAL	No
011	prflrb	Radar wind profiler from Multi-Agency Profiler (MAP) Sodar wind profiler - acoustic sounder (SODAR) winds	No
012	rass	Temperature profiles from wind profiling radars with Radio Acoustic Sounding Systems (RASS) components	No
013	prflrj	Japanese Meteorological Agency profiler winds	No
014	prflrh	Other profiler winds	No
016	prflre	European profiler winds	No

Table 6. EMC operational data inventory for vertical soundings from profilers: wind direction and speed from Radar and Sodar; temperatures from Radar with RASS).

Quality control is a significant challenge with radar observations and includes deliasing, clutter removal algorithms, and mitigating impacts from biological contamination. Without bird migration detection and removal, observations can have significant bias during migratory seasons. Thus, for their effective use, Doppler radar observations must undergo strict quality control (Liu et al. 2016).

At present, the most common method employed in operations for radar reflectivity assimilation involves converting reflectivity to a latent heating rate (Benjamin et al. 2016). This latent heating rate is then applied during a short period of time in the model initialization process (e.g. nudging), and replaces the heating tendencies coming from the model's microphysics scheme. This approach has the advantage of being inexpensive to apply, making it well-suited for applications with exceptionally low latency. The impact of this technique is relatively short lived, with improvements in forecasts lasting 6-12 hours as depicted in Figure 6.

However, more recent work has shown that direct assimilation of radar reflectivity in a 3D Ensemble-Variational framework ultimately produces a superior forecast relative to nudging (Duda et al. 2019). Building on those results, direct assimilation (Wang and Wang 2017) was recently introduced into operations with the HRRRv4 data assimilation system, a first step toward replacing the older nudging approach in the operational suite.

Radial wind assimilation was first attempted in real time as a part of a demonstration for the 1996 Atlanta Olympics and was later introduced into NCEP operations with the Eta model. To date, assimilation of radial winds has led to mostly neutral impacts - likely owing to relatively coarse resolution of the modeling systems and challenging quality control. However, as spatiotemporal resolution continues to increase, and our data assimilation systems improve, such observations may have greater impact. Indeed a recent study has shown that radial wind

observations can have a positive impact when super-observation parameters appropriate for the convective-scale are used (e.g. Lippi et al. 2019).

In addition to Doppler radial velocities, one may also derive Velocity Azimuth Display (VAD) wind profiles from a single radar. VAD winds provide wind information similar to that provided from a wind profiler. In data denial experiments by James and Benjamin (2017) they showed that VAD wind observations yielded generally positive forecast impact, except at times during which biological contamination was likely present (e.g. bird migration). VAD winds are used in both global and regional data assimilation systems.

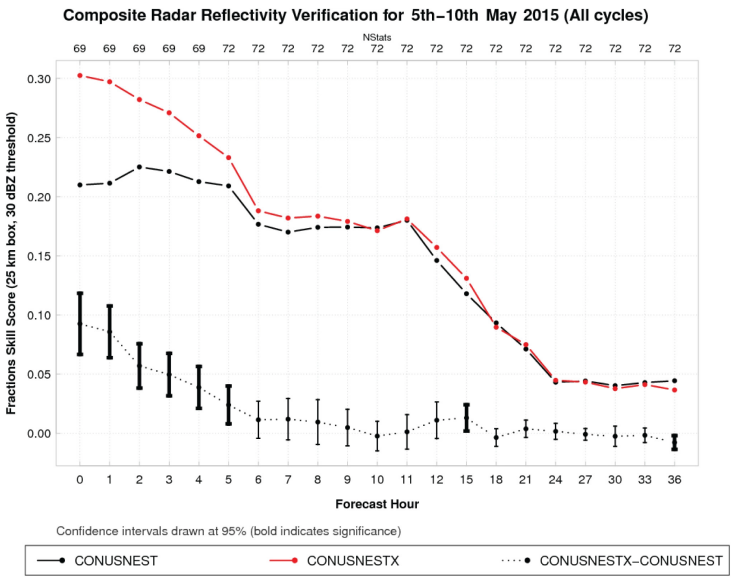

Figure 6. Fractions Skill Score shown for two experiments running without (black) and with (red) radar-derived latent heat nudging. The difference between the two is shown in the dotted line with bold confidence intervals indicating statistically significant differences at the 95% level. Figure is adapted from Gustafsson et al. (2018).

BUFR Type 006 Radar Data Doppler Radar			
Subtype	**Mnemonic**	**Description**	**Restricted**
010 - 033	rd2wxx	NEXRAD radial wind (Level II) - hourly	No
040 - 063	rd2rxx	NEXRAD reflectivity (Level II) - hourly	No
080 - 103	rdcwxx	Canadian radar radial wind - hourly	Yes
110 - 133	rdcrxx	Canadian radar reflectivity - hourly	Yes

Table 7. EMC operational data inventory for Doppler radar: radial wind and reflectivity.. xx: start time (UTC) of the measurement (e.g., 01 represents the measurement from 0100 - 0159 UTC)

BUFR Type 002 Vertical Soundings Doppler Radar			
Subtype	**Mnemonic**	**Description**	**Restricted**
008	nxrdw	NEXRAD Velocity Azimuth Display (VAD) winds decoded from radar coded message	No
017	nxrdw2	NEXRAD Velocity Azimuth Display (VAD) winds generated from Level II decoder	No
018		Other radar Velocity Azimuth Display (VAD) winds (e.g., from Europe, New Zealand)	No

Table 8. EMC operational data inventory for vertical soundings: Doppler radar-derived wind speed and direction.

4.3.3 Lightning

There are several ground based lightning detection networks, most maintained by commercial entities (e.g. Earth Networks' Total Lightning Network or Vaisala's National Lightning Detection Network). These consist of numerous distributed antennas that can measure the location, polarity, and intensity of lightning strikes (both intra-cloud and cloud-to-ground). In regional applications lightning data fills an important gap in the radar network by providing observations of deep convective storms in regions that are poorly sampled by conventional means, such offshore and in complex terrain (e.g., Rudlosky et al. 2020). In regional, high resolution data assimilation applications lightning flash density is converted into a proxy radar reflectivity which is then assimilated.

4.4 Remotely sensed (satellite data)

In current NCEP operational systems, satellite data assimilated are from three types of satellite systems: polar-orbiting (sun-synchronous; low earth orbit), geostationary and the global navigation satellite system (GNSS). The polar-orbiting satellites operate in three orbit types (early AM, mid-AM, and PM; Figure 7). The constellation of polar-orbiting satellites ensures that data from any region of the Earth are no more than 6 hours old. The 3-orbit backbone provides full global coverage in a 6-hour assimilation window (Figure 8) and significantly contributes to forecasting skills. One thing to note is that the microwave (MW) sounders on legacy POES satellites are still operationally assimilated even though they are operating beyond their planned mission life. They are still providing valuable data and positively impacting NWP model performance. The geostationary satellites from GOES, Meteosat, and Himawari programs are valuable for NWP applications because satellites in this orbit provide a constant view of the same surface area and the constellation of these satellites provides full global coverage up to latitudes of 60 degrees. Geostationary satellites send information about clouds, water vapor, and wind every few minutes. This near-constant stream of information serves as the basis for most weather monitoring and forecasting. The radio occultation measurement from GNSS is a satellite remote sensing technique that uses GNSS measurements received by low-Earth

orbiting satellites to profile the Earth's atmosphere and ionosphere with high vertical resolution and global coverage.

This section will discuss the current use of satellite data, including radiances from Infrared and MW sensors, satellite-derived winds, and radio occultation from GNSS in the NCEP global operational system. Tables 9-15 document the inventory of the remotely sensed data from three types of satellite systems and their usage in the NCEP operational global DA system, respectively.

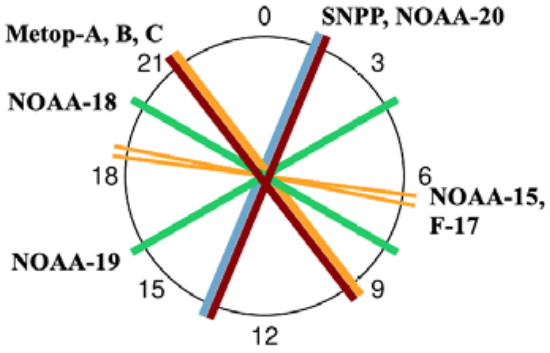

Figure 7. Equatorial crossing time of various polar-orbiting satellites that are currently operational. The orbits continue to drift, and the equator times shown are valid for mid-2018 (Source: Bormann et al., 2022, ECMWF).

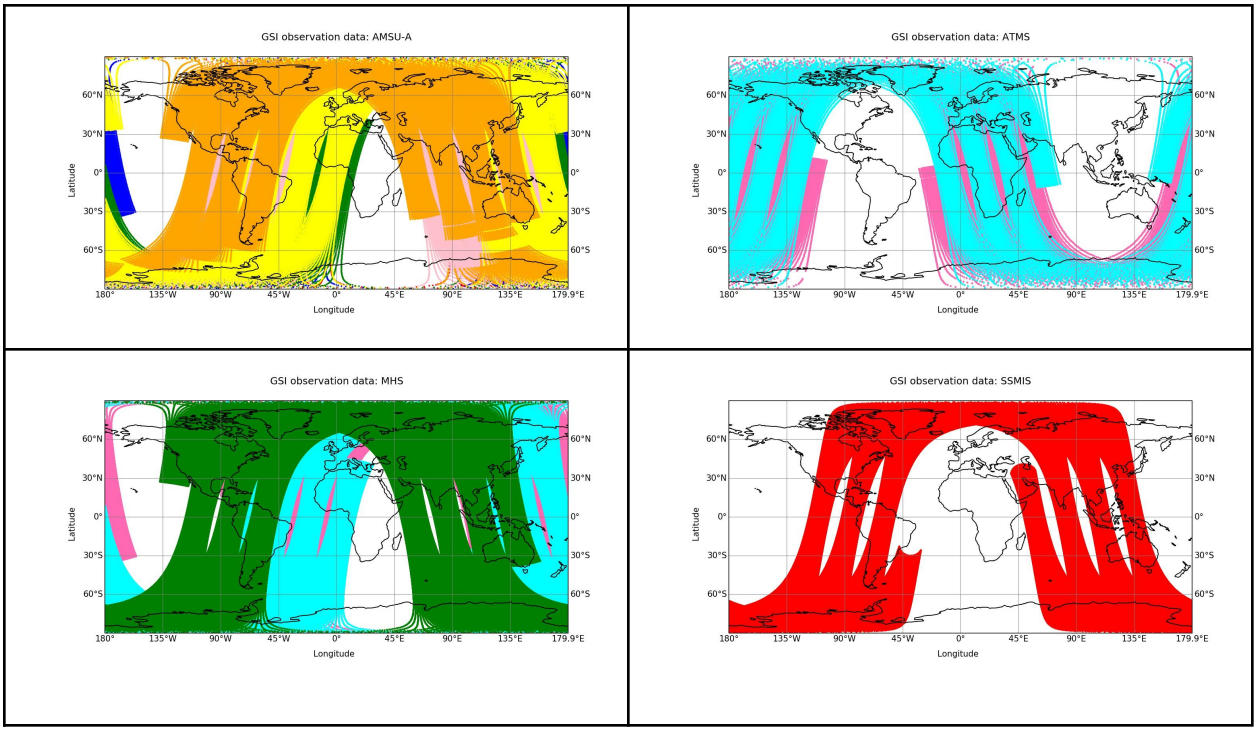

Figure 8. Spatial coverage for MW data in a 6-hour window.

4.4.1 Infrared Radiances

Infrared radiometers used in NWP sample the spectrum between 3 and 15μm. This spectrum is divided into the following broad regions (see Figure 9):

1. The 15μm CO_2 v_2 absorption feature. This primarily provides information on the atmospheric temperature profile. The central feature of this band (the Q-branch) contains information on stratospheric and mesospheric temperatures.
2. The 4.3μm CO_2 v_2 absorption feature. This also provides information on the atmospheric temperature profile but, due to interference from solar radiation and difficulties modeling non local thermal equilibrium effects, this region has not thus far been used extensively in NWP.
3. The 6.3μm H_2O v_2 absorption feature. This is the primary source of water-vapor information in the spectrum. There is significant interference from CH_4 absorption in the longwave half of this feature, so channel selection here needs to take this into account.
4. The longwave window region. This comprises surface-sensitive channels plus absorption from the water vapor continuum that potentially provides information on low-level humidity.
5. The 10μm O_3 absorption feature which provides limited O_3 profile information, including at night when UV ozone sensors cannot function.
6. The shortwave window. This also provides surface information, but is affected by solar radiation and measurements are noisier for most infrared sounders.

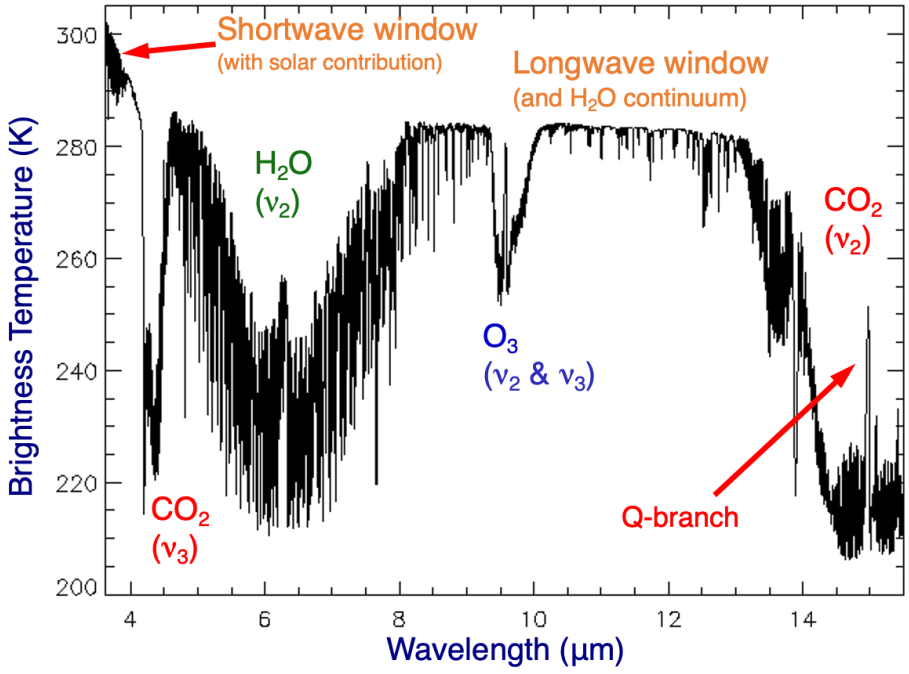

Figure 9. An example of a clear sky infrared spectrum from IASI with the main spectral features identified.

A number of trace gas features are also present in the spectrum including the aforementioned CH_4, as well as CO, N_2O, CCl_4, CFCs, HNO_3, NO_2, OCS, NO and SO_2. Infrared radiances are currently used in operational DA either from hyperspectral sounders in low-earth orbit or geostationary imagers with around a dozen channels. In both cases data volumes are such that thinning strategies (spectral and spatial thinning for the hyperspectral sounders and super-obbing for the imagers) are required to allow the data to be utilized.
Currently, the hyperspectral sounders' channels are selected to heavily favor the 15μm CO_2 v_2 band, which primarily provides information on the atmospheric temperature field, with channels also assimilated in the longwave window, ozone and water vapor bands. Only clear sky radiances are operationally assimilated at present, with cloud detection based on Eyre and Menzel (1989). Clear channels are assimilated, so high-peaking channels may be assimilated in cloudy regions if they are not sensitive to the levels with clouds.

Most satellite instruments are assimilated assuming that the observation errors are spectrally independent, i.e. the observation error covariance matrix is diagonal ("observation error" here refers not just to the instrument error, but other sources in the O-B calculation including forward model error and representativeness error but excluding model error) . These observation errors are often inflated to account for the true, correlated nature of the observation errors thereby potentially under-weighting the data in the assimilation system. Spectrally correlated observation errors have been introduced to the GSI in recent years (e.g., Bathmann and Collard, 2021) for IASI and CrIS (see Figure 10 as example) which use error estimation procedures introduced by Desrosiers et al. (2005). Although the Desrosiers technique is considered a superior method for estimating observation errors, tuning is still required to ensure positive impact and to ensure the observations error covariance matrix is not ill-conditioned.
The geostationary infrared imagers are assimilated via a clear sky radiance (CSR) product where a segment array of pixels (15x15 for ABI, 16x16 for SEVIRI And Himawari) are combined, retaining only the clear scenes. This reduces the very large data volumes from these satellites as well as reducing the effective noise. At present only water vapor channels are assimilated in this way. A summary of the infrared radiances that are assimilated into the GFS can be found in Tables 9 & 10.

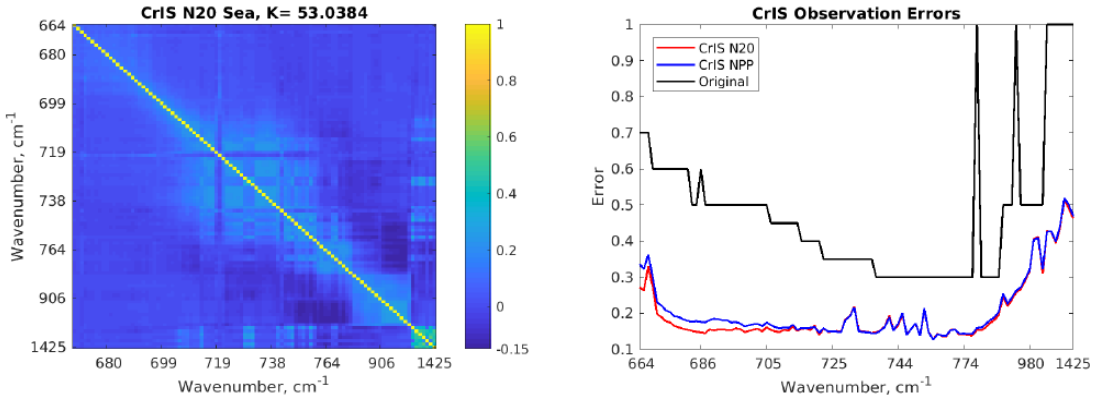

Figure 10. CrIS NOAA-20 error correlation matrix over sea (left) and observation errors for CrIS NOAA-20 and S-NPP compared to original errors that do not account for correlations (right). Figures adapted from Bathmann and Collard (2021).

Instrument	Platforms	Type	Channels Assimilated
CrIS	SNPP, JPSS-1, JPSS-2	LEO hyperspectral sounder	84 Channels
IASI	Metop-B,C	LEO hyperspectral sounder	165 Channels
SEVIRI	Meteosat-8,11	Geostationary imager	5,6 (6.2 & 7.3μm)
ABI	GOES-16	Geostationary imager	8,10 (6.2 & 7.3μm)
AHI	Himawari-9	Geostationary imager	8,9,10 (6.2, 7.0 & 7.3μm)

Table 9. Summary of infrared radiances assimilated in the Global Forecast System.

Satellite	Sensor		Satellite	Usage
Microwave Polar-Orbiting	**AMSU-A**	Advanced Microwave Sounding Unit - A	NOAA-15 NOAA-18 NOAA-19 MetOp-B MetOp-C AQUA	Radiance All-sky
	MHS	Microwave Humidity Sounding	MetOp-B MetOp-C	Radiance
	ATMS	Advanced Technology Microwave Sounder	NOAA-20 S-NPP	Radiance All-sky
	SSMIS	Special Sensor Microwave - Imager/Sounder	DMSP-16 DMSP-17 DMSP-18	Radiance
Infrared Polar-Orbiting	**IASI**	Infrared Atmospheric Sounding Interferometer	MetOp-B MetOp-C	Radiance
	CrIS	Cross-track Infrared Sounder	NOAA-20 S-NPP	Radiance
	VIIRS	Visible/Infrared Imager Radiometer suite	NOAA-20 S-NPP	Radiance
	AVHRR/3	Advanced Very High Resolution Radiometer / 3	MetOp-B MetOp-C	Radiance
Infrared Geostationary	**ABI**	Advanced Baseline Imager	GOES-16 GOES-18	Radiance (Clear-sky Radiance Product)
	SEVIRI	Spinning Enhanced Visible Infra-Red Imager	MeteoSat-08 MeteoSat-09 MeteoSat-10 MeteoSat-11	Radiance (Clear-sky Radiance Product)
	AHI	Advanced Himawari Imager	Himawari-8 Himawari-9	Radiance (Clear-sky Radiance Product)

Table 10. List of Radiance data used in NCEP operational global DA system.

4.4.2 Microwave Radiances

4.4.2.1 Data Coverage

Microwave measurements make a major contribution to the observing system, which are routinely assimilated into models to determine the initial conditions for the weather forecast. Operational microwave radiances in NCEP data assimilation systems are from a 3-orbit constellation (see Table 10; Figures 7 & 8) operated by POES, JPSS, EUMETSAT, and DMSP programs. These microwave observations have been the most impactful remote sensing observations in the numerical weather prediction models for the past two decades (Eyre et al. 2021).

4.4.2.2 Channels

The current NCEP operational data assimilation system assimilates microwave-sounding channels ranging from 23 to 183 GHz, sensitive to the surface, temperature, moisture, and hydrometers with an all-sky approach treating clear and cloudy scenes together. The channel selection for the current microwave sounders is based on the absorption feature of oxygen in the 50-60 GHz region, which provides temperature information and water vapor in the 23 and 183 GHz regions. Channels at 23.8, 31.4, and 165.5 GHz are used for inferring clouds, hydrometeors, and surface parameters. Among these operational MW sounders, the assimilation of the AMSU-A and ATMS radiances is under an all-sky framework, whereas MHS and SSMIS are still used under clear-sky conditions only. Figure 11 and Table 11 summarize the channel characteristics of these operational MW sensors.

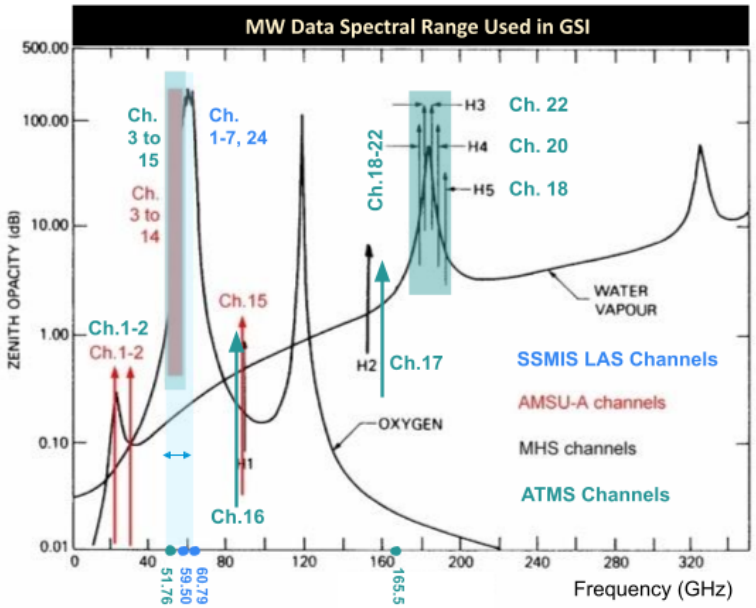

Figure 11. Channel center frequencies of ATMS, AMSU-A, MHS, and SSMIS overlaid on the absorption spectra of oxygen and water vapor in the atmosphere.

4.4.2.3 Forecast Impact

The all-sky framework gives a wider observational coverage (Figure 12) and brings information on water vapor, temperature, and clouds from MW observations into the analysis, benefiting forecasts. The all-sky framework has removed a spurious low-level moisture bias caused by the earlier clear-sky framework and improved forecast scores (Zhu et al. 2016). The ensemble forecast sensitivity to observation impact (EFSOI) study performed at the time when the AMSU-A all-sky framework was operational indicated that the AMSU-A observation has a significant positive total impact per cycle to 24-hour forecast error reduction (Figure 13). The tropospheric channels are beneficial to forecast error reduction with the greatest impact from channel 6 (54.4.GHz) peaking at 300 hPa (see Figure 14, left panel). Statistically, most of the AMSU-A observations show benefits to 24-hour forecast error reduction except for some locations at higher latitudes associated with storm tracks (Figure 14).

Sensor	Platform	Window	WV 23	Window 31	Oxygen 49-70	Window 89	Window 150-165	WV 183-190	Notes
AMSU-A	NOAA-15 NOAA-18 NOAA-19 MetOp-B MetOp-C		23.8 V	31.4 V	50.3000 V 52.8000 V 53.5960 H 54.4000 H 54.9400 V 55.5000 H 57.2903 H (6)	89.0 V			All-sky
ATMS	S-NPP NOAA-20		23.8 QV	31.4 QV	53.3000 QH 51.7600 QH 52.8000 QH 53.5960 QH 43.4000 QH 54.9400 QH 55.5000 QH 57.2903 QH (6)	89.5 QV	165.5 QH	183.31 QH (5)	All-sky
MHS	NOAA-19 MetOp-B MetOp-C					89 V	157 V	183.31 H (2) 190.31 V	Clear-sky
SSMIS	DMSP-F17	19.35 V 19.35 H	22.235 V	37.0 V 37.0 H	50.300 H 52.800 H 53.596 H 54.500 H 55.500 H 57.290 RC 59.400 RC 60.792 RC (5) 63.238 RC	91.65 V 91.65 H	150 H	183.31 H (3)	Clear-sky

Table 11. List of MW sensors, platforms, and channel information used in the operational DA system.

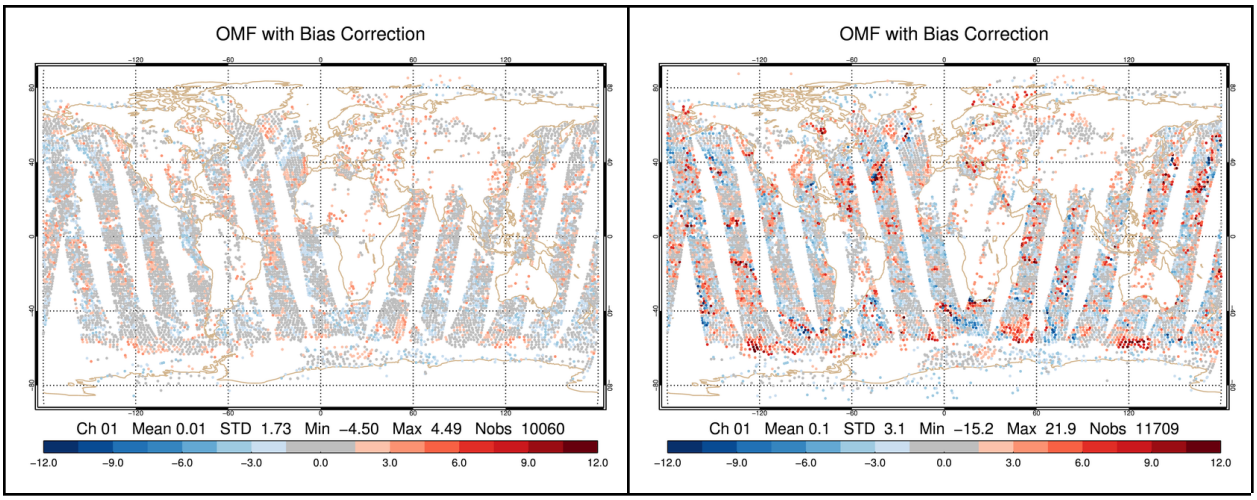

Figure 12. Spatial distribution of the innovation with bias correction for AMSU-A data passed quality control under clear (left panel) and all-sky (right panel) conditions.

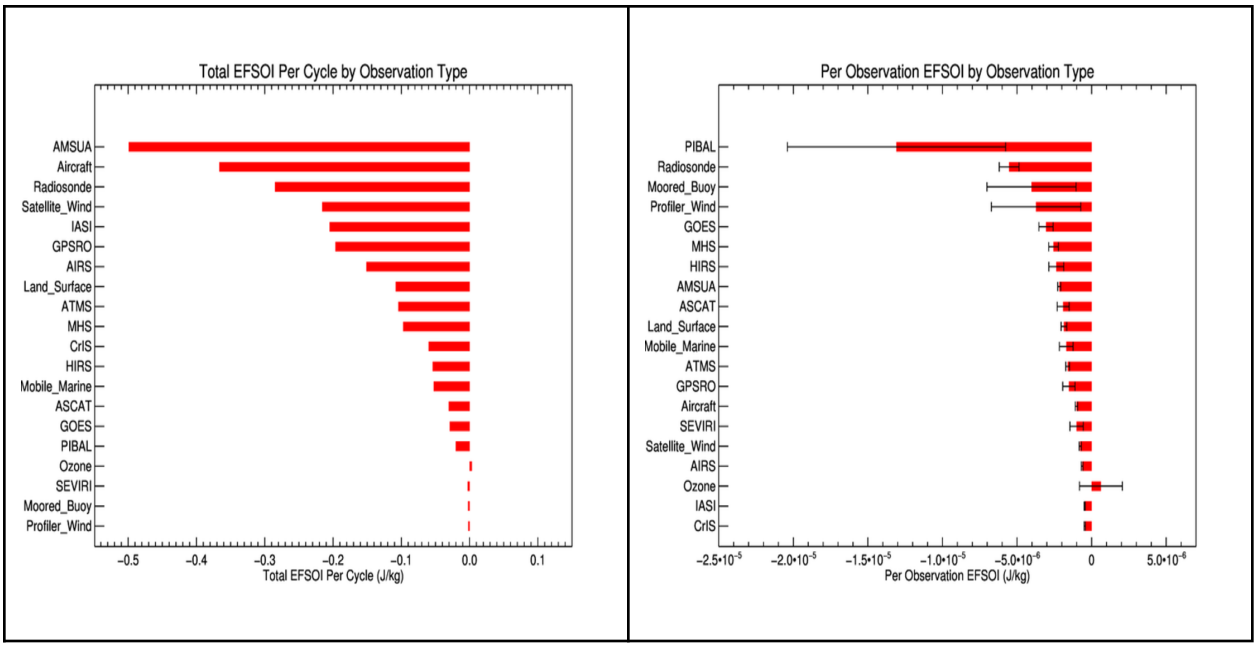

Figure 13. Ensemble forecast sensitivity to observation impact: total (left panel) and per observation (right panel) impact by observation type.

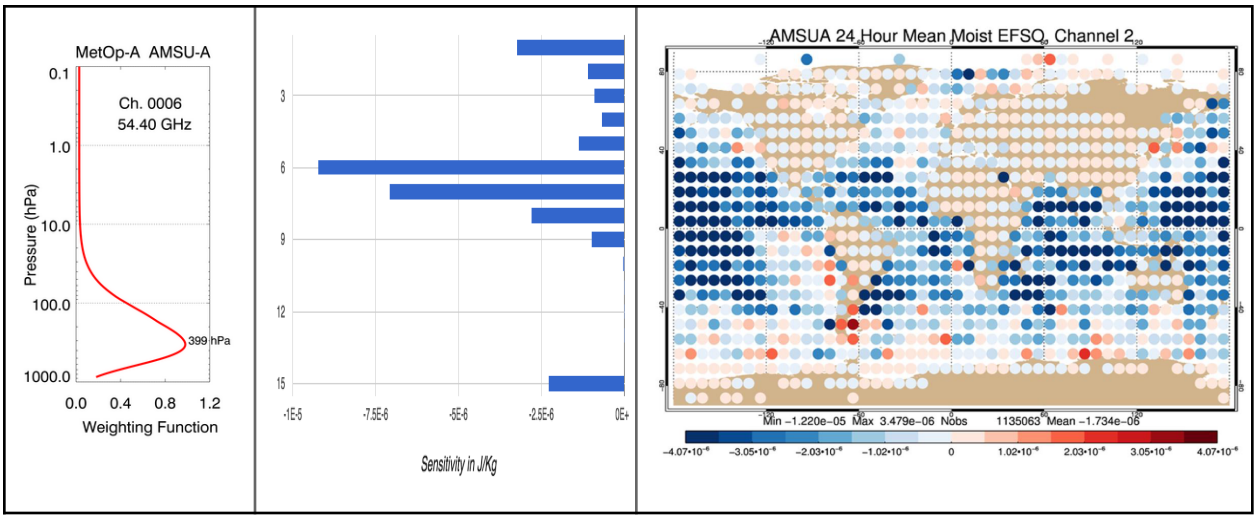

Figure 14. Ensemble forecast sensitivity to observation impact: total impact per AMSU-A channel (middle), impact from AMSU-A channel 2 (right), and the weighting function for AMSU-A channel 6 (left).

4.4.2.4 Pioneering All-sky Microwave Assimilation

Before 2017, the operational systems assimilated MW radiances in clear-sky conditions. Data affected by thick clouds and precipitation were excluded before the assimilation, and the effect of thin clouds in the data was removed through variational bias correction. The development of the all-sky framework made the assimilation of cloud-affected, non-precipitating radiances from AMSU-A and ATMS possible (Zhu et al. 2016; Zhu et al. 2019). As a result, more data are assimilated in regions where active weather conditions occur (Figure 12). The GFS under a clear-sky framework has been known to overestimate the stratus clouds along the continental western coasts. The all-sky approach reduces the relative humidity analysis at 850 hPa and correspondingly increases the temperature analysis at the same level.

The operational all-sky assimilation features are summarized in terms of the observation and analysis perspectives, respectively.

All-sky approach - observation perspective:

- Use both clear and non-precipitating cloud-affected AMSU-A and ATMS radiances over the ocean; clear-sky radiance only over non-ocean surfaces.
- Include cloud liquid water and cloud ice (non-precipitating hydrometeors) in the observation operator over the ocean to calculate the simulated radiances and Jacobians.
- Screen out observations containing precipitation. Various measurements of the scattering effect from precipitation hydrometeors are applied to identify data affected by precipitation. Figure 15 illustrates a complete ATMS quality control flowchart, including the precipitation screening based on the scattering effect.
- Model observation errors as a function of symmetric cloud amount to ensure Gaussianity of the observation error as proposed by Geer and Bauer (2011); Geer et al. (2012). Compute the standard deviation of the first-guess departures as a function of the

averaged cloud amount estimated from observation and background, respectively (Figure 16)

- Situation-dependent observation error inflation. Additional inflation is constructed empirically based on the assumption that the observation error has a dependency on the physical parameters that are sensitive to the observation operator. Similar to variational quality control, the purpose of the additional inflation is to ensure that radiances with large first-guess departures can still be used in the analysis with reduced weights while not shocking the system. The situation-dependent error inflation significantly improves wind forecast in the tropospheric winds for both hemispheres.
- No bias correction based on cloud liquid water over the ocean (the simulated observations now include the effect of cloud).
- Assume cloudy scenes are overcast.

All-sky approach - analysis perspective:

- The control variable is total cloud condensate (CW: sum of cloud liquid water and cloud ice).
- The splitting of total cloud condensate into cloud liquid water and ice is a function of air temperature.
- Set the standard deviation of the static background error for CW to 5% of its first guess. The static error covariance does not provide the cross-covariances between CW and other control variables. Flow-dependent error covariances, including cross-covariances, are estimated from ensemble forecasts, which plays a more important role in the analysis.
- Bias correction estimate uses data passed quality control with consistent cloud information in the observation and forecast. Samples with conflicting cloud information within the field of view, such as clear forecast versus cloudy observation, are not used to estimate bias correction.
- The use of the cloud control variable allows the cloud information from radiances mapped to temperature and moisture fields and cloud fields directly.
- Additional cloud analysis increments are generated from the projection of the radiance information onto the cloud fields through the background error variances for clouds and the background error cross-covariance.
- No hydrometer increments for forecast initialization.
- Use 4D-incremental Analysis Update (4D IAU, Lei and Whitaker 2016) to propagate increments in the assimilation window to reduce the spin-down issue commonly observed in the initialization for hydrometers.

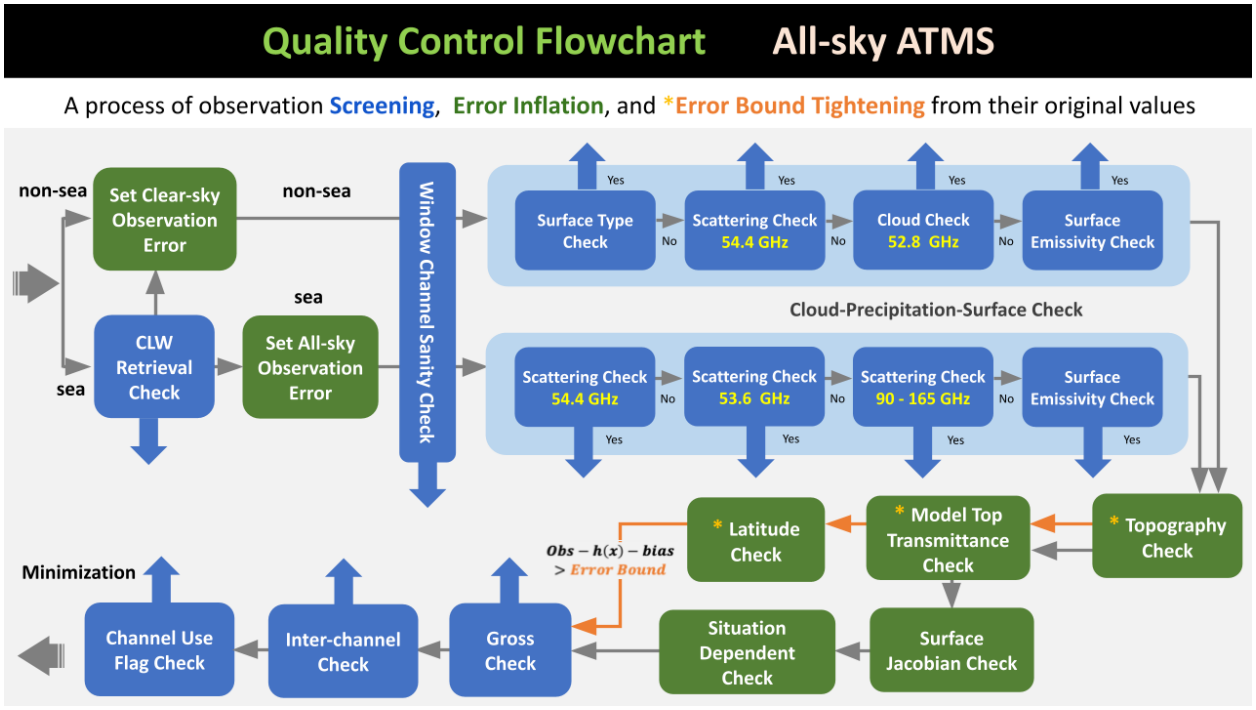

Figure 15. Quality control procedure for ATMS radiance under all-sky conditions.

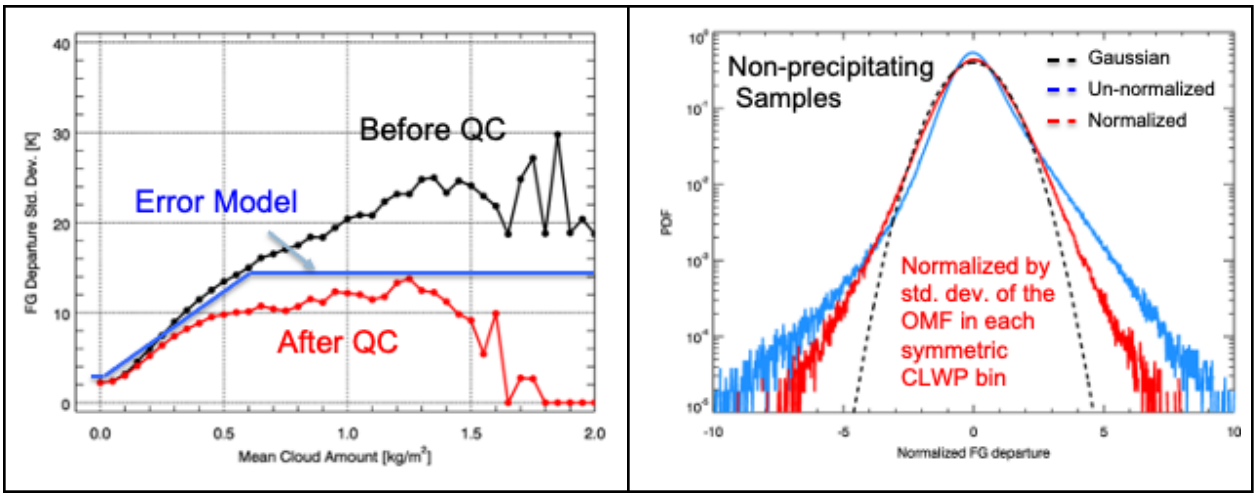

Figure 16. Left panel: the standard deviation of the first-guess departure before (black) and after (red) quality control calculated from the experiment cycles between 1 to 15 Nov 2013 and the assigned symmetric observation error (K, blue) for AMSU-A NOAA-19 channel 1 with respect to the mean cloud amount (k gm^{-2}). Right panel: the normalized (red) and unnormalized (blue) PDFs of the first-guess departure after quality control, and the Gaussian PDF (black).

4.4.2.5 Evolution of GDAS and MW data

Figure 17 documents the evolution of GDAS and the use of MW data over the years.

The contributions already made and in progress towards the success of all-sky MW radiance assimilation in GDAS are summarized as the following:

- Improvement in the forecast model
  - Resolution - higher horizontal and vertical resolution, and raised model top
  - Representation of cloud and moisture processes
  - Initialization technique
- Advanced data assimilation techniques
  - Flow-dependent background error covariance through the use of ensemble
  - Representation of model uncertainties through stochastic physics
  - Situation dependent observation error model
- More accurate radiative transfer modeling
  - Scattering by hydrometeors
  - Subgrid variability or cloud and precipitation overlap
  - Simulation under fractional cloud coverage

One reason to assimilate cloud and precipitation-sensitive observations is simply to make better use of existing data. Current NCEP operational systems only assimilate radiances from selected MW sounders (ATMS and AMSU-A). No data from MW imagers sensitive to moisture and clouds are used.

ECMWF (Duncan et al. 2021) recently performed observing system experiments (OSEs) to examine the addition of MW temperature and humidity sounders from a baseline with no MW sounder at all, showing the incremental benefit of adding sounders to the assimilation system (Figure 18). The addition of MW sounders causes a significant increase in NWP skill, and the impact is largest in the stratosphere but is visible for all parameters and levels analyzed. The largest impacts are obtained from the first sounders added. A further benefit is observed from additional sounders, and no saturation is evident in the maximal setup.

The addition of MW imagers such as AMSR-2 and GMI is also beneficial to the forecast (Kazumori et al. 2016; Lean et al. 2017). In addition, pioneering work at ECMWF to extend the all-sky framework to include all-surface assimilation had been implemented for SSMIS on DMSP F-17, which has near-global utilization including ocean, sea-ice, and land including snow-covered land surfaces (Geer 2013; Baordo and Geer 2016).

The pathway for developing MW radiance data for NCEP operational systems in the near-term is clear. The next step is to include MW radiances from existing imagers such as GMI, AMSR-2, and SSMIS. For the longer term, many new observations giving information on clouds and precipitation, such as the Ice Cloud Imager that observes selected frequencies between 183 GHz and 664 GHz (sub-mm range), cloud lidar, and radar, will be available in the next two decades. The pathway to enhance the current all-sky framework, including the observation operator, is discussed in the 10-year data assimilation strategy document (Kleist et al. 2023).

Year	1991	1995	1998	2007	2012	2014	2016	2019	2021
Analysis	Spectral Statistical Interpolation (SSI)			Gridpoint Statistical Interpolation (GSI)					
Algorithm	3DVar				Hybrid, 3DEnVar T574/T254 L64 EnSRF, 80 ensembles		Hybrid, 4DEnVar T574/T574 (39 km) L64 EnSRF, 80 ensembles	Hybrid, 4DEnVar T766/T766 (25 km) L64 EnSRF, 80 ensembles	Hybrid, 4DEnVar T766/T766 (25 km) L127 LETKF, 80 ensembles
Balance				Tangent-linear Normal Model Constraint (TLNMC)					
Satellite Data	NESDIS Retrievals	• Direct Radiance Assimilation • Clear-sky Radiance Assimilation					• Direct Radiance Assimilation • All-sky Radiance Assimilation for AMSU-A (2016) and ATMS (2019) • Non-precipitating cloud affected radiances are assimilated		
Obs Operator				CRTM Scattering Solver Advanced Doubling & Adding Method (ADA)			CRTM with Scattering Solver (ADA) + Simulation under Fractional Cloud Coverage (2017) • Cloud Overlap (Total Cloud Cover) • Two-column Radiance Calculation		
Bias Correction	Offline	Two-step Bias correction • VarBC for air-mass predictors • Time-moving average of O-F for scan angle predictors				Variational Bias Correction (VarBC) for all predictors			
Forecast	Spectral Model Sigma Eulerian T126 L18 (1991) L28 (1993)	Spectral Model Hybrid Semi-Lagrangian (2007) Zhao-Carr Microphysics (cloud water and ice) T170 (105km) L42 (1998) T574 (23km) L64 (2010)					Spectral Model Hybrid Semi-Lagrangian Zhao-Carr Microphysics T1534 (13km) L64, Model Top 55km	FV3 Dynamic Core GFDL Microphysics 5 Hydrometers T1534 (13km) L64, Model Top 55km	FV3 Dynamic Core GFDL Microphysics 5 Hydrometers T1534 (13km) TL127, Model Top 80km
Initialization				Digital Filter Initialization (DFI)				No DFI	4D Incremental Analysis Update (IAU)

Figure 17. Evolution of GDAS and the use of MW data over the years.

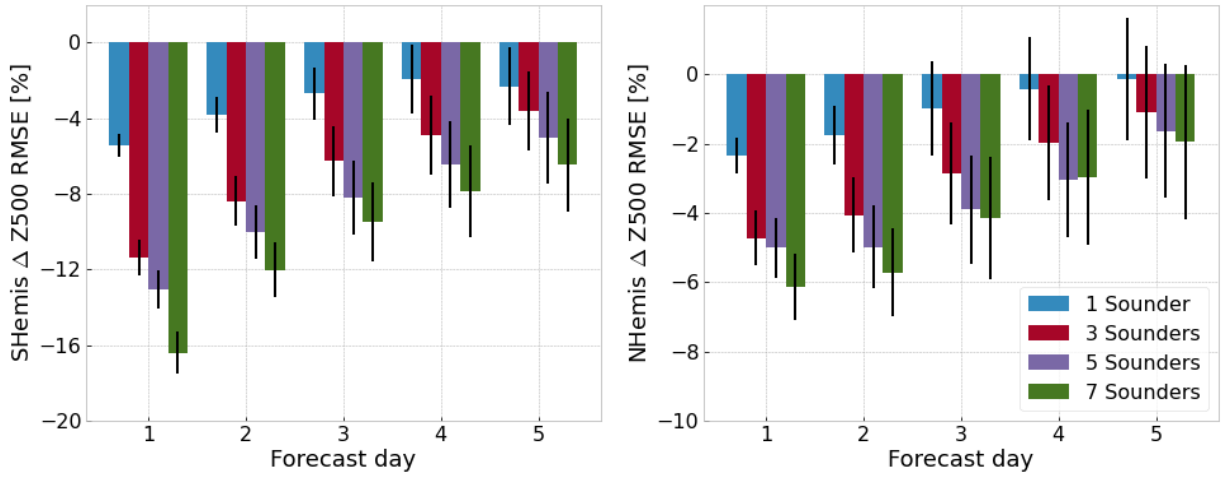

Figure 18. 500 hPa geopotential height RMSE change relative to no sounders from day 1 to day 5 in two regions: Southern Hemisphere (left) and Northern Hemisphere (Right). From Duncan et al. 2021.

4.4.3 Satellite-derived winds

Satellite wind observations are either in the form of derived motion winds (DMWs); retrievals from scatterometry measurements; or, most recently, doppler wind lidar. Most of these types of observations that are currently assimilated in the GSI at NCEP are DMVs - where atmospheric features (usually clouds, but clear sky winds are derived from tracking features in water vapor imagery) are tracked in successive images to infer the wind field. These are derived products that are supplied by the respective space agencies.

Scatterometry winds are also derived products. Scatterometers are active remote sounding systems where the backscatter from a microwave radar pulse from the ocean surface at various azimuth angles is used to infer sea-state and hence the near surface wind field.

The experimental Aeolus satellite from the Atmospheric Dynamics Mission contains a first ever space-based doppler wind lidar that provides line-of-sight wind information. While this is assimilated at some NWP centers, the expected short lifetime of this instrument and lack of a follow-on mission resulted in the decision to not assimilate these data operationally in the GSI. There was substantial development work completed within GSI and the observation operator is readily available (Apodaca et al. 2023; Marinescu et al. 2022).

Satellite	Sensor		Satellite	Usage
Polar-Orbing NOAA	AVHRR/3	Advanced Very High Resolution Radiometer / 3	NOAA-15 NOAA-18 NOAA-19 MetOp-B MetOp-C	Wind derivation by tracking clouds and water vapor features
	VIIRS	Visible/Infrared Imager Radiometer Suite	NOAA-20 NPP	Wind derivation by tracking clouds and water vapor features
	MODIS	Moderate-resolution Imaging Spectro-radiometer	TERRA AQUA	Wind derivation by tracking clouds and water vapor features
	ASCAT	Advanced Scatterometer	MetOp-B MetOp-C	Sea surface wind vector
Geostationary	ABI	Advanced Baseline Imager	GOES-16 GOES-18	Wind derivation by tracking clouds and water vapor features
	SEVIRI	Spinning Enhanced Visible Infra-Red Imager	MeteoSat-08 MeteoSat-09 MeteoSat-10 MeteoSat-11	Wind derivation by tracking clouds and water vapor features
	AHI	Advanced Himawari Imager	Himawari-8 Himawari-9	Wind derivation by tracking clouds and water vapor features

Table 12. List of satellite winds used in NCEP operational global DA system.

	Observation Type					
Satellite/ Instrument	Water Vapor Cloud Top	Water Vapor Clear Air Deep Layer	Shortwave Infrared Cloud Top	Longwave Infrared Cloud Top	Visible Cloud Top	Scatterometer
Geostationary:						
GOES-16/ABI	✓	✓		✓		
GOES-17/ABI	✓	✓		✓		
Himawari-8/AHI	✓	✓		✓	✓	
Meteosat-8/Seviri	✓			✓	✓	
Meteosat-11/Seviri	✓	✓		✓	✓	
Polar:						
Terra/MODIS	✓	✓		✓		
Aqua/MODIS	✓	✓		✓		
NOAA-15/AVHRR				✓		
NOAA-18/AVHRR				✓		
NOAA-19/AVHRR				✓		
Metop-B/AVHRR				✓		
SNPP/VIIRS				✓		
JPSS-1/VIIRS				✓		
Metop-B/ASCAT						✓

Table 13. Use of satellite winds based on platform, sensor, and spectral type.

4.4.4 Ozone

Apart from the information contained in the infrared radiances, the ozone analysis is constrained through the use of retrievals from ultraviolet ozone sounders. Retrievals are assimilated from the S-NPP OMPS (both nadir profile and total column) as well as the total column product from OMI on EOS-Aura (this latter instrument was launched in 2004). The OMPS total column product from NOAA-20 has been assimilated since November 2022.

Additional instruments exist, in particular GOME-2 on Metops -A and -C, MLS on Aura and TROPOMI on Sentinel 5-P, and nadir-profiler and limb-profilers on NOAA-20 which are not assimilated due to inconsistencies between the products.

Ozone retrievals are assimilated using a simple observation operator (effectively treating the retrieval as an ozone sonde and ignoring the finite vertical resolution of the product) and assuming that the observations are unbiased. Explicit treatment of the vertical resolution of the products through the use of averaging kernels in the observation operator, plus the introduction of bias correction could greatly improve the exploitation of these data sources. It is important to note that while the 3D ozone fields are updated throughout the global atmospheric model, the focus has been on improving the representation of stratospheric ozone for its impact on radiative forcing (and in turn satellite radiances) and not tropospheric ozone for near-surface air quality applications.

Space Agency	Sensor		Satellite	Usage
NOAA **POES** **Polar Operational Environmental Satellites**	**SBUV/2**	Solar Backscatter Ultraviolet /2	NOAA-15 NOAA-18 NOAA-19	Ozone profile
NOAA **JPSS** **Joint Polar Satellite System**	**OMPS-limb**	Ozone Mapping and Profiler Suite	S-NPP Not on NOAA-20	Stratospheric ozone profile
	OMPS-nadir	Ozone Mapping and Profiler Suite	NOAA-20 S-NPP	Ozone profile
			NOAA-20 S-NPP	Total-column ozone
EUMETSAT **EPS** **EUMETAT Polar System**	**GOME-2**	Global Ozone Monitoring Experiment - 2	MetOp-B MetOp-C	Ozone profile and Total-column ozone
NASA **EOS** **Earth Observation System**	**OMI**	Ozone Monitoring Instrument	AURA	Total-column ozone
	MLS	Microwave Limb Sounder	AURA	Ozone profile and Total-column ozone

Table 14. List of ozone data used in NCEP operational global DA system.

4.4.5 GNSS-RO

Another form of satellite retrievals are radio occultations (RO), derived through the use of Global Navigation Satellite System (GNSS) transmitters. These observations are often referred to as GNSS-RO or GPS-RO (named for the North American-centric Global Positioning System, which

is included within GNSS). When a GNSS radio wave signal moves through the atmosphere, the trajectory is refracted or bent by the varying densities of the air it passes through, this results in a small but measurable delay (microseconds) in the arrival time of the signal. The signal is intercepted by a receiver on board a low Earth orbit (LEO) satellite, from which the time delay of the original signal can inform the thermodynamic properties of the part of the atmosphere that it traversed (see Figure 19). These raw phase delay measurements can be processed through a number of levels that rely on progressively more a priori assumptions. These are bending angle profiles; refractivity profiles and ultimately geophysical profiles (temperature and humidity). Eyre (1994) discusses approaches for assimilating refractivity profiles and bending angles into an NWP system.

The GSI has previously assimilated refractivity observations, but with the adoption of a new forward operator in 2012, NCEP's Bending Angle Method (NBAM, Cucurull et al. 2013), NCEP transitioned to assimilating bending angles instead.

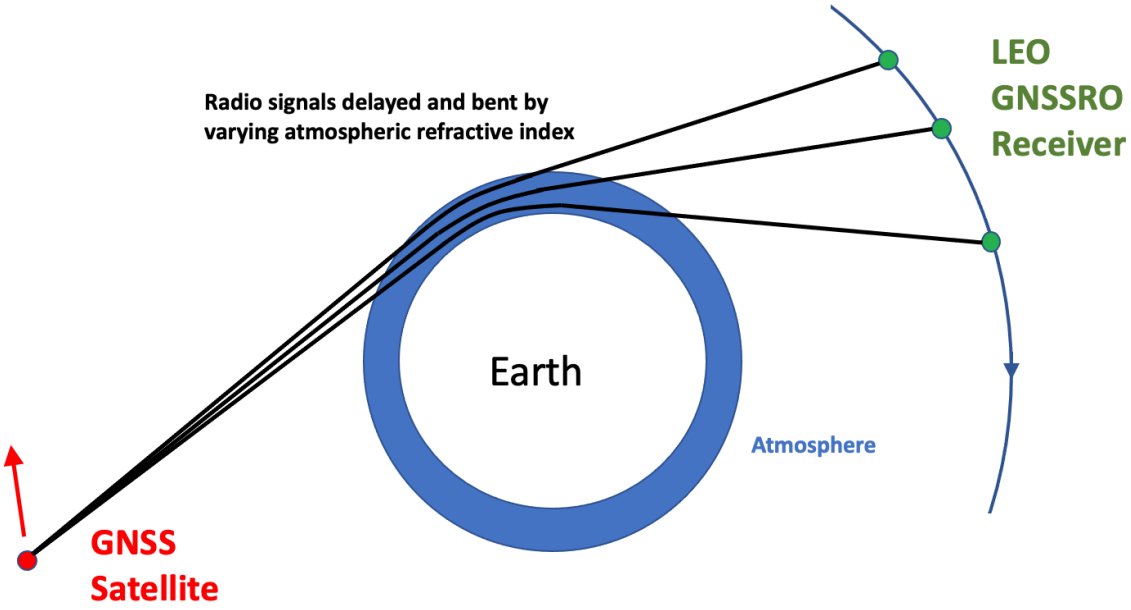

Figure 19. Schematic of the geometry of a GPSRO profile observation.

GNSS-RO observations provide extensive coverage of the atmosphere, with no impact from clouds or the underlying land surface. Apart from providing information on temperature and humidity, GNSS-RO observations can also serve as an anchor for the variational bias correction of other observations being that they are largely unbiased. The first demonstration mission was the GPS-Met mission launched in 1995. Today, one of the primary sources of currently assimilated GNSS-RO data is COSMIC-2, a joint US-Taiwan venture that consists of six LEO satellites, providing over 5,000 occultations per day, mostly concentrated in the tropics and subtropics. When first operationally assimilated, COSMIC-2 provided more occultations than all other missions combined. Observations from COSMIC-2 are also of high quality with a high

signal to noise ratio and deeper penetration into the troposphere compared to other RO observations (Shao et al. 2023). More recently, NESDIS and EUMETSAT are purchasing GNSS-RO observations from commercial vendors such as PlanetIQ and Spire Global (and previously GeoOptics) for operational assimilation as part of their Commercial Weather Data Programs. Other GNSS-RO platforms currently assimilated in operations include the MetOp constellation, TerraSar-X, TANDEM-X, and KOMPSAT-5 (see Table 15 and Figure 20).

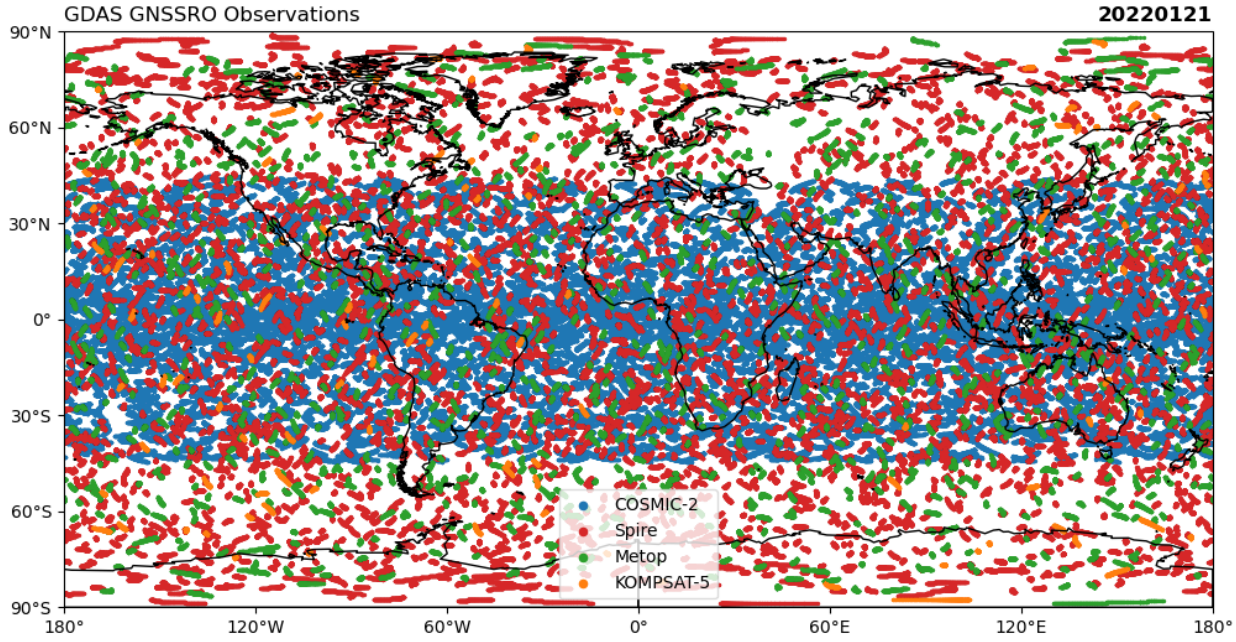

Figure 20. Global coverage of select GNSSRO observations assimilated into the GDAS for one day (January 21, 2022) colored by constellations (COSMIC-2: blue; Spire: red; Metop: green; KOMPSAT-5: orange).

4.4.6 Ground-based GNSS & PWAT Retrievals

The ground-based GNSS network represents a source of precipitable water retrievals that can be assimilated for atmospheric NWP (e.g. Wolfe and Gutman 2000). To generate these retrievals we leverage the measurable signal delays between GNSS satellites and ground-based receivers. These delays may be generally explained by a relatively stable hydrostatic delay alongside a more variable wet delay. The wet delay corresponds to atmospheric water vapor content, and with this knowledge we may then derive the precipitable water (e.g. Bevis et al. 1992).

NOAA's rapidly updated regional atmospheric prediction system assimilates approximately 700 of these precipitable water retrievals per analysis. Data denial work by James and Benjamin (2017) has shown that these precipitable water observations have a small but positive impact on short term forecasts from NOAA's Rapid Refresh (RAP) forecast system.

Future priorities are shifting toward the assimilation of the zenith total delay as opposed to the retrievals. Zenith total delay conveniently does not require co-located observations of surface pressure and thus allows for additional observations to be assimilated. An early example of assimilation of this type of observation into a variational assimilation system is reported in De Pondeca and Zou (2001).

Space Agency Probram	Sensor		Satellite	Usage
EUMETSAT **EPS** EUMETSAT Polar System	**GRAS**	GNSS Receiver for Atmospheric Sounding	MetOp-B MetOp-C	Bending Angle
NASA **GRACE Follow-on** Recovery and Climate Experiment	**Tri-G**	Triple GPS	GRACE-FO (2 sats)	Bending Angle
KARI **KOMPS** Korea Multi-Purpose Satellite	**AOPOD**	Atmosphere Occultation and Precision Orbit Determination	KOMPSAT-5	Bending Angle
NSPO/NOAA/UCAR **COSMIC** Constellation Observing System for Meteorology and	**TGRS**	Tri-GNSS Radio Occultation System	COSMIC-2 (FormoSat)	Bending Angle
DLR (Germany) **TerraSAR**	**TerraSAR**	Tracking, Occlusion and Ranging	TerraSAR-X	Bending Angle
			TanDem-X	Bending Angle
MDE (Spain) **SEOSAR/PAZ** Satellite Español de Observación SAR (PAZ)	**ROHPP**	Radio Occultations and Heavy Precipitation with PAZ	SEOSAR/PAZ	Bending Angle
GeoOptic **CICERO** Community Initiative for Continuing Earth Radio Occultation	**CION**	CICERO Instrument for GPS-RO	CICERO	Bending Angle
SPIRE **Low Earth Multi-Use Receiver**	**STRATRO**	STRATOS	Lemur-2	Bending Angle

Table 15. List of radio occultation data used in NCEP operational global DA system.

4.4.7 Radar altimetry

Along with the remotely sensed observation in the MW and IR band that are sensitive to the ocean and sea-ice and are described previously, radar altimetry is an important source of information for the ocean and cryosphere. It is the primary source of information for ocean circulation, ocean thermal and haline content, ocean volume, sea-ice volume and significant wave height. Most of the altimeters currently operating are ingested and assimilated into marine systems, including CryoSat-2, Jason-3, Sentinel-3A, Sentinel-3B and Sentinel-6A Michael Freilich (Jason-CS).

5 Assimilation Monitoring and Observation Impacts

Given the tremendous volume of data that is processed and assimilated for any individual cycle, along with the complexity of modern data assimilation systems, regular monitoring and automated alerts are critical for detection of potential issues and assessing the need for intervention. While quality control plays an important role in catching data that should not be assimilated, there are many circumstances for which intervention is necessary to start rejecting entire classes of observations, e.g. for satellite channels/platforms going bad, etc. Further, it is important to regularly monitor things like data counts (see Figure 21), innovation statistics, etc. to observe the overall health of the system. NCEP currently has several automated tools to assist with monitoring and alerting to operational issues. The tools are designed to monitor aspects of the assimilated observations as well as things like the behavior of the solver (e.g. variational minimization). The current set of tools have been developed and accumulated over the years, and need to be reimagined through the lens of future needs and infrastructure. New capabilities that are being developed as part of the JEDI transition and acceptance process will be the foundation for a future, holistic approach to operational assimilation monitoring.

In addition to internal monitoring of observation quality and assimilation performance, there is regular exchange of information across the international NWP community. This includes things like regular publication and sharing of reject lists, notifications when particular systems (such as individual satellites or channels) have issues or go bad, or anomalous performance of particular subsets of observations. There is also additional information produced and provided to the WMO Integrated Global Observing System (WIGOS) Data Quality Monitoring System (WDQMS). This is a relatively new system under the WMO with a growing set of observations being reported upon.

The ability to assess and understand the impact of assimilation of observations for improving the analysis and reducing forecast error is another important element, not only for monitoring system performance, but informing how to optimize the system in a holistic manner. At present, there are two approaches that are currently taken to assess the impact of observations or analysis quality in operational systems at NCEP. The first approach is to perform Observing System Experiments (OSEs), also known as data addition or denial experiments. While straightforward to do and interpret, these are computationally expensive. A second approach, cross-validation, has been utilized to assess the quality of analysis in the RTMA/URMA by

withholding subsets of data through offline analysis or as part of the outer loop configuration. While both of these approaches are useful, there are new techniques available to add to the toolkit for assessing the assimilation of observations including Analysis/Forecast Sensitivity to Observations Impact (ASOI/FSOI), ensemble variance reduction methods (Harnisch et al. 2013). The use of ASOI/FSOI, in particular, has become standard practice at many operational centers. Preliminary versions of GSI-based Ensemble FSOI (EFSOI) have already been developed and are being matured as an interim solution, while investment in JEDI-based FSOI is being pursued in parallel as part of the future capabilities. A concerted effort will be made to expand and build a monitoring toolkit that will be applied, and unified, for assimilation components across the spectrum of UFS-based systems.

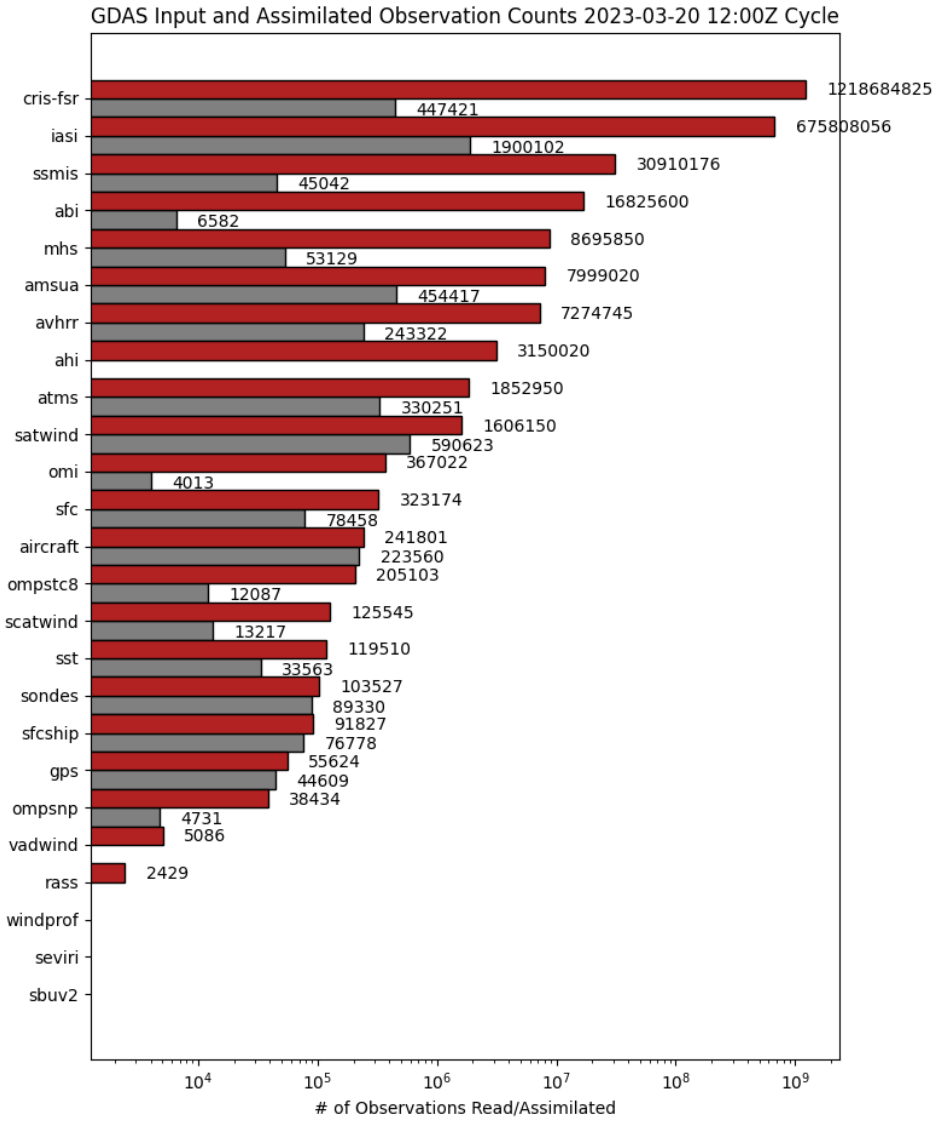

Figure 21. Total number of observations available to (red) and used by (gray) the GSI for each observation type for the GDAS analysis cycle valid March 20, 2023 12 UTC. Note the x-axis is on a logarithmic scale.

6 Current Implementation Procedure

The process of implementing DA changes into NCEP operations involves several steps. Specific steps vary based on the nature of the changes to be implemented. For example, assimilating a new observation type involves more steps than updating the variational solver within the DA application. Figure 22 shows the typical implementation steps when adding a new observation type. Other changes to the DA system will usually skip steps 1-4a and, instead, begin with 4b.

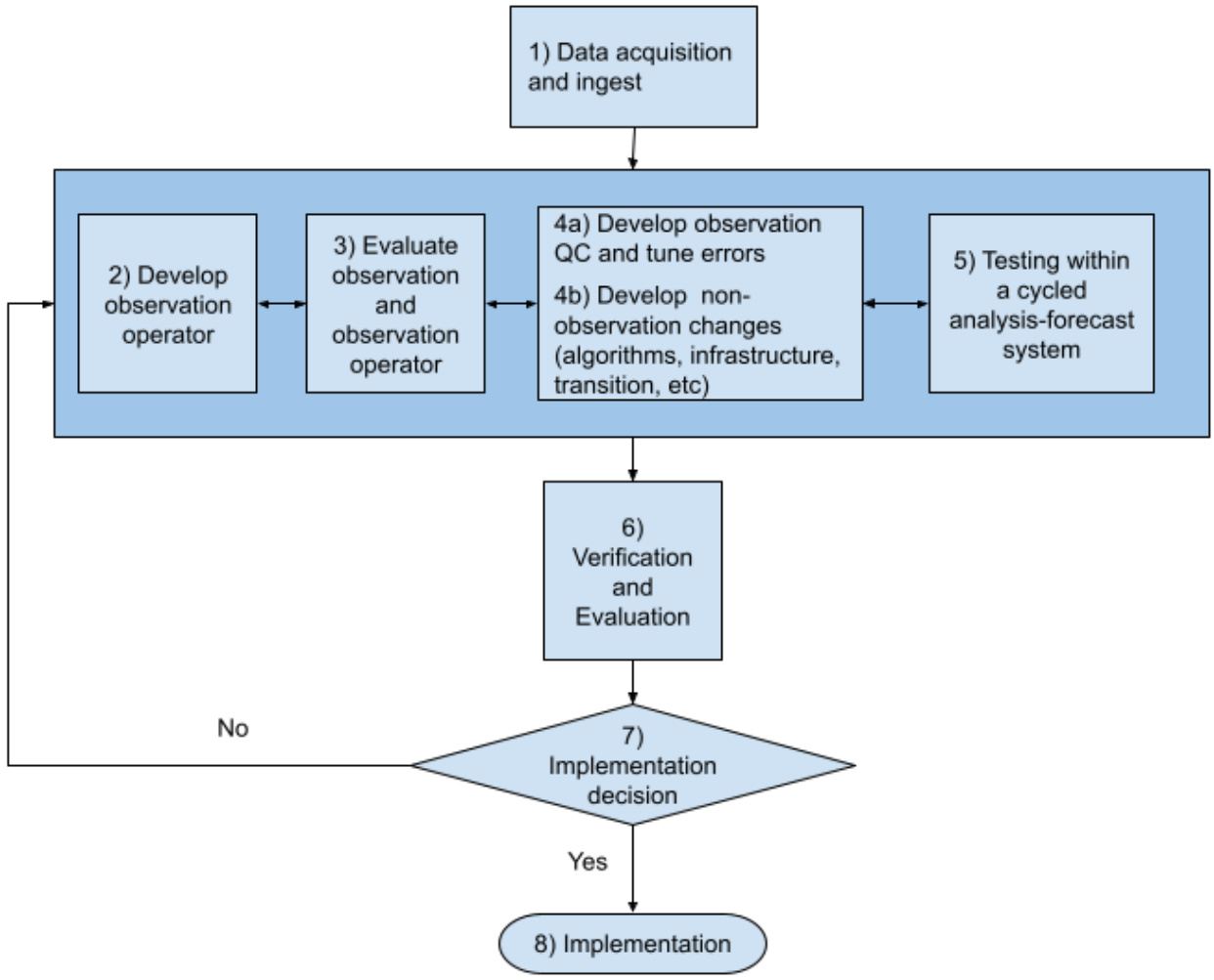

Figure 22. Flowchart depicting the iterative process by which new observations are implemented into an operational data assimilation system.

The steps for an observation upgrade are expanded upon below.

1) *Data acquisition and ingest*
   For any observation to be assimilated, a reliable data stream must be set up to prepare the data for use in DA. Observations are typically provided in BUFR format - the WMO standard - but alternative methods may be acceptable for non-operational datasets. Timeliness, the time from data collection and transmission to ingest and preparation for use by DA, is a critical factor. Operational DA systems run with strict data cutoff windows. Late arriving data will not be assimilated in real-time. Such data, however, may still be of use for reanalysis or verification.

2) *Development of the observation operator*
   Prior to deployment or launch, every instrument needs to be characterized and calibrated so that the observation operator (and its adjoint) and error model can be developed. The observation operator simulates observation values from model fields. For example, the Community Radiative Transfer Model (CRTM) simulates radiances from model predicted states. New satellite sensors require instrument spectral response functions in order for the CRTM to simulate the given data.

3) *Evaluate observations and observation operator*
   Although the instrument behavior should be well-characterized before deployment, it is still necessary to evaluate the instrument's performance within the context of the DA system. Comparison of observation operator simulated values with the observations inform quality control and bias correction decisions as well as evaluating the full error budget. These comparisons provide vital feedback on the quality of the observations, observation operator, and input model fields.

4) *Development of observation quality control, error tuning and/or other algorithm changes*
   The evaluation of the instrument performance at the monitoring stage is combined with expert knowledge of the expected characteristics of the instrument and forward operator to design quality control, bias correction and observation error assignment strategies. The concern here is not just errors in the observations themselves, but also the ability to model them. For example, with radiance data it is usual to either remove observations that are affected by clouds or to inflate errors in those situations to reflect the fact that cloudy radiative transfer is more challenging than for clear sky. The error characterization needs to include all aspects, including instrumentation, forward model, and representativeness errors.

   DA development also includes improvements to DA infrastructure or algorithms (see sections 3 and 4). Other DA implementations address technical changes instead of focusing on infrastructure or science upgrades. Technical implementations include transition to new operational computing environments, updates to support software, changes in data format, etc.

5) *Testing within a cycled analysis-forecast system*
The full data assimilation and forecast system must be cycled for a sufficiently long time to generate robust statistics documenting the impact of observation or algorithm changes on analysis and forecast performance. "Sufficient duration" refers not only to the length of a given continuously cycled test but also to tests over different seasons (e.g, meteorological winter and summer).

Some analysis and forecast systems have extensive downstream dependencies (e.g., GFS). Changes to such systems require downstream applications to also be tested and evaluated in either cycled mode or for select time periods.

The entire testing process requires considerable computational resources and staff commitment over an extended period. These resource demands, both staff and machine, often compete with other evaluations, computational constraints, and other projects. The availability of these resources is the biggest single factor in ensuring a timely implementation of a new observation or other DA changes.

6) *Verification and Evaluation*
Analysis and forecast performance from the cycled system is evaluated using a variety of objective metrics. These metrics compare output against assimilated and independent observations as well as cycled and independent model fields. Subjective evaluations (case studies, mean states, etc) are conducted by developers and/or customers. If DA changes impact downstream applications, output from the downstream systems also needs to be examined and evaluated. All verification, evaluations, and customer feedback is collected into summary reports for presentation to management.

7) *Implementation decision*
Verification feedback informs management's decision to move forward with the proposed changes or identifies areas that require additional work. In the later case development returns to one of the previous steps.

8) *Implementation*
Pending management's decision to move forward with the proposed changes, the package is prepared for operational implementation. DA implementations are often bundled with other changes. EMC staff work across branches to prepare tags, bundle components, prepare release notes, and ensure compliance with NCEP Central Operations (NCO) implementation standards. NWS notifications, with various time leads, must be published informing NWS and external customers of upcoming changes. Some of these notices may be disseminated earlier in the implementation process.

NCO staff receive the full implementation package and perform infrastructure testing. Noted issues are returned to developers to be addressed and updates are passed back to NCO. Large implementation packages (e.g., GFS) often require NCO to run multi-week real-time parallels prior to implementation. Issues with the computational environment, critical weather days, instrument failures, or other unforeseen events can

delay, possibly derail, implementations. As such there can be a sizable time delay between delivery of implementation packages and the actual implementation. During this delay at least a portion of DA staff time is dedicated to monitoring the pre-implementation package and responding to issues as they arise.

Implementing changes into operational NCEP DA systems is a multistep process involving a wide range of subject matter experts (internal, cross agency, and external collaborators) along with the consumption of considerable computational and storage resources. These realities expand implementation timelines. While consolidating NWS NWP systems reduces the number of systems to update, the increasing complexity of the remaining NWP systems requires detailed upgrade plans with well defined deliverables, clear decision points, and dedicated staff and computer resources. Research and development on cutting edge science involves a degree of uncertainty which must be accounted for in project plans. Balancing this with the incremental yet steady implementation of innovations presents challenges. This speaks to both the science and art of operational NWP.

7 Summary

This document presents an overview of the past and present operational data assimilation capabilities at NWS/NCEP. The data assimilation infrastructure has evolved over the years, including an initial foray into unification across applications and embracing of community development through the GSI. Similar to other centers, NCEP embraced variational data assimilation and expanded to the incorporation of ensembles for prescribing background error covariances. Separately, several developments have occurred to enable assimilation for non-atmospheric data assimilation systems such as the implementation of capabilities for the RTOFS system. A new era is being envisioned as developments are now underway to work toward further unification of infrastructure to enable coupled assimilation for UFS-based applications. This document also provided a thorough review of the utilization of the global observing system and outline of current implementation procedures.

For decades, NCEP has been a world leader in operational NWP, pioneering advancements at global and regional scales, encompassing a whole suite of forecast applications that have data assimilation components. With that legacy in mind, a companion document (Kleist et al. 2023) has been created that will serve as a roadmap for the next decade of progress in data assimilation here at NCEP. Building off of the material presented here, with this 10 year strategy, NCEP will have the vision outlined to continue to be a world leader in DA and NWP.

References

Apodaca, K., L. Cucurull, I. Genkova, R. J. Purser, and X. Su, 2023: Assessing the benefit of variational quality control for assimilating Aeolus Mie and Rayleigh wind profiles in NOAA's global forecast system during tropical cyclones. Quart. J. Roy. Meteorol. Soc., 1-23, https://doi.org/10.1002/qj.4530.

Bannister, R. N., 2016: A review of operational methods of variational and ensemble-variational data assimilation. *Quart. J. Roy. Meteorol. Soc.,* **143**, 607-633, https://doi.org/10.1002/qj.2982.

Baordo, F. and A. J. Geer, 2016: Assimilation of SSMIS humidity-sounding channels in all-sky conditions over land using a dynamic emissivity retrieval. *Quart. J. Roy. Meteorol. Soc.,* **142**, 2854–2866, https://doi.org/10.1002/qj.2873.

Bauer, P., A. Thorpe, and G. Brunet, 2015: The quiet revolution of numerical weather prediction. *Nature*, **525**, 47–55, https://doi.org/10.1038/nature14956.

Behringer, D. W., M. Ji, and A. Leetmaa, 1998: An Improved Coupled Model for ENSO Prediction and Implications for Ocean Initialization. Part I: The Ocean Data Assimilation System. *Mon. Wea. Rev.*, **126(4)**, 1013-1021, https://doi.org/10.1175/1520-0493(1998)126%3C1013:AICMFE%3E2.0.CO;2.

Behringer, D. W., 2007: The Global Ocean Data Assimilation System (GODAS) at NCEP. Preprints, *11th Symp. on Integrated Observing and Assimilation Systems for Atmosphere, Oceans, and Land Surface*, San Antonio, TX, Amer. Meteor. Soc, 3.3, http://ams.confex.com/ams/pdfpapers/119541.pdf.

Benjamin, S. G., T. G. Smirnova, E. P. James, L. F. Lin, M. Hu, D. D. Turner, and S. W. He, 2022: Land-Snow Data Assimilation Including a Moderately Coupled Initialization Method Applied to NWP. *J. Hydrometeor.*, **23**, 825-845, https://doi.org/10.1175/Jhm-D-21-0198.1.

Benjamin, S. G., and Coauthors, 2021: Stratiform Cloud-Hydrometeor Assimilation for HRRR and RAP Model Short-Range Weather Prediction. *Mon. Wea. Rev.*, **149**, 2673-2694, https://doi.org/10.1175/MWR-D-20-0319.1.

Benjamin, S. G., and Coauthors, 2016: A North American Hourly Assimilation and Model Forecast Cycle: The Rapid Refresh. *Mon. Wea. Rev.*, **144**, 1669-1694, https://doi.org/10.1175/MWR-D-15-0242.1.

Bathmann, K., and A. Collard, 2021: Surface-dependent correlated infrared observation errors and quality control in the FV3 framework, *Quart. J. Roy. Meteor. Soc.*, **147**, 408–424, https://doi.org/10.1002/qj.3925.

Bevis, M., S. Businger, T. A. Herring, C. Rocken, R. A. Anthes, and R. H. Ware, 1992: GPS meteorology: Remote sensing of atmospheric water vapor using the global positioning system. *Journal of Geophysical Research: Atmospheres*, **97**, 15787-15801, https://doi.org/10.1029/92JD01517.

Bloom, S. C., L. L. Takacs, A. M. da Silva, and D. Ledvina, 1996: Data Assimilation Using Incremental Analysis Updates. *Mon. Wea. Rev.*, **124**, 1256–1271, https://doi.org/10.1175/1520-0493(1996)124<1256:DAUIAU>2.0.CO;2.

Bormann, N., B. Bell, D. Duncan, S. English, A. Geer, K. Lean, and F. Prates, 2021: Use and impact of MW sounders at ECMWF and perspectives for future systems. Presentation for NOAA Microwave Sounder Workshop, July 28, 2021, College Park, MD.

https://www.nesdis.noaa.gov/s3/2022-03/Bormann_20210728_MW_sounder_Workshop_Metoffice.pdf.

Brennan, M. J., D. T. Kleist, K. Howard, and S. J. Majumdar, 2015: The impact of supplemental dropwindsonde data on the structure and intensity of Tropical Storm Karen (2013) in the NCEP Global Forecast System. *Wea. Forecasting*, **30**, 683-691, https://doi.org/10.1175/WAF-D-15-0002.1.

Buizza, R., M. Miller, and T. N. Palmer, 1999: Stochastic Representation of model uncertanties in the ECMWF Ensemble Prediction System. *Quart. J. Roy. Meteor. Soc.*, **125**, 2887–2908, https://doi.org/10.1002/qj.49712556006.

Craven, J.P., D.E. Rudack, and P.E. Shafer, 2020: National Blend of Models: A statistically post-processed multi-model ensemble. *J. Operational Meteor.*, **8**, 1–14, https://doi.org/10.15191/nwajom.2020.0801.

Cucurull, L., J. C. Derber, and R. J. Purser, 2013: A bending angle forward operator for global positioning system radio occultation measurements. *Journal of Geophysical Research: Atmospheres*, **118(1)**, 14-28, https://doi.org/10.1029/2012JD017782.

De Pondeca, M. S. F. V., and Coauthors, 2011: The Real-Time Mesoscale Analysis at NOAA's National Centers for Environmental Prediction: Current Status and Development. *Wea. Forecasting*, **26**, 593-612, https://doi.org/10.1175/WAF-D-10-05037.1.

De Pondeca, M. S. F. V., and X. Zou, 2001: A Case Study of the Variational Assimilation of GPS Zenith Delay Observations into a Mesoscale Model, *J. Appl. Meteor. Climatol.*, **40(9)**, 1559-1576, https://doi.org/10.1175/1520-0450(2001)040%3C1559:ACSOTV%3E2.0.CO;2.

Derber, J., and A. Rosati, 1989: A Global Oceanic Data Assimilation System, *J. Phys. Oceanogr.*, **19(9)**, 1333-1347, https://doi.org/10.1175/1520-0485(1989)019%3C1333:AGODAS%3E2.0.CO;2.

Derber, J. C., and W.-S. Wu, 1998: The Use of TOVS Cloud-Cleared Radiances in the NCEP SSI Analysis System, *Mon. Wea. Rev.*, **126(8)**, 2287-2299, https://doi.org/10.1175/1520-0493(1998)126%3C2287:TUOTCC%3E2.0.CO;2.

Derber, J. C., Parrish D. F., and Lord S. J. , 1991: The new global operational analysis system at the National Meteorological Center. *Wea. Forecasting*, **6**, 538–547, https://doi.org/10.1175/1520-0434(1991)006%3C0538:TNGOAS%3E2.0.CO;2.

Duda, J. D., X. Wang, Y. Wang, and J. R. Carley, 2019: Comparing the Assimilation of Radar Reflectivity Using the Direct GSI-Based Ensemble–Variational (EnVar) and Indirect Cloud Analysis Methods in Convection-Allowing Forecasts over the Continental United States, *Mon. Wea. Rev.*, **147(5)**, 1655-1678, https://doi.org/10.1175/MWR-D-18-0171.1.

Duncan, D. I., N. Bormann, and E. V. Hólm, 2021: On the addition of microwave sounders and numerical weather prediction skill. *Quart. J. Roy. Meteor. Soc.*, **147**, 3703-3718, https://doi.org/10.1002/qj.4149.

Eyre, J.R., 1994: Assimilation of radio occultation measurements into a Numerical Weather Prediction System. *ECMWF Tech. Memo.,* 199, 35 pp., https://doi.org/10.21957/r8zjif4it.

Eyre, J. R., and W. P. Menzel, 1989: Retrieval of cloud parameters from satellite sounder data: A simulation study. *J. Appl. Meteor.*, **28**, 267–275, https://doi.org/10.1175/1520-0450(1989)028%3C0267:ROCPFS%3E2.0.CO;2.

Eyre, J., W. Bell, J. Cotton, S. English, M. Forsythe, S. Healy, and E. Pavelin, E, 2021: Assimilation of satellite data in numerical weather prediction. Part II: recent years. *Quart. J. Roy. Meteor. Soc.,* 521– 556, https://doi.org/10.1002/qj.4228.

Gamache, J. F., F. D. Marks, and F. Roux, 1995: Comparison of Three Airborne Doppler Sampling Techniques with Airborne In Situ Wind Observations in Hurricane Gustav (1990). *J. Atmos. Oceanic Technol.*, **12**, 171-181, https://doi.org/10.1175/1520-0426(1995)012<0171:COTADS>2.0.CO;2.

Geer, A., 2013: All-sky assimilation: better snow-scattering radiative transfer and addition of SSMIS humidity sounding channels. *ECMWF Tech. Memo.,* 706, 26 pp., https://doi.org/10.21957/uxq5zlprk.

Geer, A. J., and P. Bauer, 2011: Observation errors in all-sky data assimilation. *Quart. J. Roy. Meteor. Soc*., **137**, 2024–2037, https://doi.org/10.1002/qj.830.

Geer, A. J., P. Bauer, and S. English, 2012: Assimilating AMSU-A temperature sounding channels in the presence of cloud and precipitation. *ECMWF Tech. Memo.,* 670, 41 pp., https://doi.org/10.21957/mbjps5x4j.

Gustafsson, N., and Coauthors, 2018: Survey of data assimilation methods for convective-scale numerical weather prediction at operational centres. *Quart. J. Roy. Meteor. Soc.,* **144**, 1218-1256, https://doi.org/10.1002/qj.3179.

Hamill, T. M., and Coauthors, 2021: The Reanalysis for the Global Ensemble Forecast System, version 12, *Mon. Wea. Rev.*,**150(1)**, 59-79, https://doi.org/10.1175/MWR-D-21-0023.1.

Harnisch, F., S. B. Healy, P. Bauer, and S. J. English, 2013: Scaling of GNSS Radio Occultation Impact with Observation Number Using an Ensemble of Data Assimilations. *Mon. Wea. Rev*., **141(12)**, 4395-4413, https://doi.org/10.1175/MWR-D-13-00098.1.

Hu, M., S. G. Benjamin, T. T. Ladwig, D. C. Dowell, S. S. Weygandt, C. R. Alexander, and J. S. Whitaker, 2017: GSI Three-Dimensional Ensemble–Variational Hybrid Data Assimilation Using a Global Ensemble for the Regional Rapid Refresh Model, *Mon. Wea. Rev*., **145(10)**, 4205-4225, https://doi.org/10.1175/MWR-D-16-0418.1.

Huang, X., and P. Lynch, 1993: Diabatic Digital-Filtering Initialization: Application to the HIRLAM Model. *Mon. Wea. Rev*., **121**, 589–603, https://doi.org/10.1175/1520-0493(1993)121<0589:DDFIAT>2.0.CO;2.

Hunt, B. R., E. J. Kostelich, and I. Szunyogh, 2007: Efficient data assimilation for spatiotemporal chaos: A local ensemble transform Kalman filter. *Physica D*, **230**, 112–126, https://doi.org/10.1016/j.physd.2006.11.008.

Ingleby, B., and Coauthors, 2020: The impact of COVID-19 on weather forecasts: A balanced view. *Geophysical Research Letters*, **48**, e2020GL090699, https://doi.org/10.1029/2020GL090699.

James, E. P., and S. G. Benjamin, 2017: Observation system experiments with the hourly updating Rapid Refresh model using GSI hybrid ensemble–variational data assimilation. *Mon. Wea. Rev*., **145**, 2897-2918, https://doi.org/10.1175/MWR-D-16-0398.1.

Jorgensen, D. P., P. H. Hildebrand, and C. L. Frush, 1983: Feasibility Test of an Airborne Pulse-Doppler Meteorological Radar. *J. Appl. Meteor. Climatol*, **22**, 744-757, https://doi.org/10.1175/1520-0450(1983)022<0744:FTOAAP>2.0.CO;2.

Kalnay, E., and Coauthors, 1996: The NCEP/NCAR 40-Year Reanalysis Project. *Bull. Amer. Meteor. Soc.*, **77(3)**, 437-472, https://doi.org/10.1175/1520-0477(1996)077%3C0437:TNYRP%3E2.0.CO;2.

Kanamitsu, M, W. Ebisuzaki, J. Woollen, S.-K. Yang, J. J. Hnilo, M. Fiorino, and G. L. Potter, 2002: NCEP-DOE AMIP-II Reanalysis (R-2). *Bull. Amer. Meteor. Soc.*, **83**, 1631-1644, https://doi.org/10.1175/BAMS-83-11-1631.

Kazumori, M., A. J. Geer, and S. J. English, 2016: Effects of all-sky assimilation of GCOM-W/AMSR2 radiances in the ECMWF numerical weather prediction system. *Quart. J. Roy. Meteorol. Soc.*, **142**, 721–737, https://doi.org/10.1002/qj.2669.

Kim, J., and Coauthors, 2022: The NOAA-NCEP 40 year Reanalysis with the Next Generation Global Ocean Data Assimilation System (NG-GODAS): 1979 to 2019, NCEP Office Note, 509, 35 pp, https://doi.org/10.25923/26ds-q363.

Kleist, D. T., J. Carley, A. Collard, E. Liu, S. Liu, C. R. Martin, C. Thomas, R. Treason, and G. Vernieres, 2023: Data assimilation strategy and development plan for NCEP's Environmental Modeling Center, *NOAA NCEP Office Note, in press, 90 pp.*

Kleist, D. T., R. Mahajan, and C. Thomas, 2018: Data assimilation in the Next-Generation Global Prediction System (NGGPS) era: Initial implementation of FV3-based Global Forecast System (GFS). *JCSDA Quarterly*, **61**, 1-9, https://doi.org/10.25923/jw00-r987.

Kleist, D. T., and K. Ide, 2015a: An OSSE-Based Evaluation of Hybrid Variational–Ensemble Data Assimilation for the NCEP GFS. Part I: System Description and 3D-Hybrid Results, *Mon. Wea. Rev.*, **143(2)**, 433-451, https://doi.org/10.1175/MWR-D-13-00351.1.

Kleist, D. T., and K. Ide, 2015b: An OSSE-Based Evaluation of Hybrid Variational–Ensemble Data Assimilation for the NCEP GFS. Part II: 4DEnVar and Hybrid Variants, *Mon. Wea. Rev.*, **143(2)**, 452-470, https://doi.org/10.1175/MWR-D-13-00350.1.

Kleist, D. T., D. F. Parrish, J. C. Derber, R. Treason, W.-S. Wu, and S. Lord, 2009a: Introduction of the GSI into the NCEP Global Data Assimilation System, *Wea. Forecasting*, **24(6)**, 1691-1705, https://doi.org/10.1175/2009WAF2222201.1.

Kleist, D. T., D. F. Parrish, J. C. Derber, R. Treadon, R. M. Errico, and R. Yang, 2009b: Improving Incremental Balance in the GSI 3DVAR Analysis System. *Mon. Wea. Rev.*, **137(3)**, 1046-1060, https://doi.org/10.1175/2008MWR2623.1.

Lean, P., A. Geer, and K. Lonitz, 2017: Assimilation of Global Precipitation Mission (GPM) Microwave Imager (GMI) in all-sky conditions, *ECMWF Tech. Memo.,* 799, 28 pp., https://doi.org/10.21957/8orc7sn33.

Lei, L., and J. S. Whitaker, 2016: A Four-Dimensional Incremental Analysis Update for the Ensemble Kalman Filter. *Mon. Wea. Rev.*, **144**, 2605-2621, https://doi.org/10.1175/MWR-D-15-0246.1.

Lei, L., J. S. Whitaker, and C. Bishop, 2018: Improving assimilation of radiance observations by implementing model space localization in an ensemble Kalman filter. *Journal of Advances in Modeling Earth Systems*, **10**, 3221– 3232, https://doi.org/10.1029/2018MS001468.

Lippi, D. E., J. R. Carley, and D. T. Kleist, 2019: Improvements to the Assimilation of Doppler Radial Winds for Convection-Permitting Forecasts of a Heavy Rain Event. *Mon Wea. Rev.*, **147**, 3609-3632, https://doi.org/10.1175/MWR-D-18-0411.1.

Liu, Q., N. Surgi, S. Lord, S., W.-S. Wu, D. Parrish, S. Gopalakrishnan, J. Waldrop, J. and J. Gamache, 2006: Hurricane initialization in HWRF model. *Preprints from The 27th*

Conference on Hurricanes and Tropical Meteorology, Monterey, CA, https://ams.confex.com/ams/pdfpapers/108496.pdf.

Liu, S., and Coauthors, 2016: WSR-88D Radar Data Processing at NCEP. *Wea. Forecasting*, **31**, 2047-2055, https://doi.org/10.1175/WAF-D-16-0003.1.

Lord, S. J., X. Wu, V. Tallapragada, and F. M. Ralph, 2023: The Impact of Dropsonde Data on the Performance of the NCEP Global Forecast System during the 2020 Atmospheric Rivers Observing Campaign. Part I: Precipitation, *Wea. Forecasting*, **38(1)**, 17-45, https://doi.org/10.1175/WAF-D-22-0036.1.

Lorenc, A. C., and M. Jardek, 2018: A comparison of hybrid variational data assimilation methods for global NWP. *Quart. J. Roy. Meteorol. Soc.,* **144**, 2748-2760, https://doi.org/10.1002/qj.3401.

Lorenc, A. C., N. E. Bowler, A. M. Clayton, S. R. Pring, and D. Fairbairn, 2015: Comparison of Hybrid-4DEnVar and Hybrid-4DVar data assimilation methods for global NWP. *Mon. Wea. Rev*., **143**, 212-229, https://doi.org/10.1175/MWR-D-14-00195.1.

Marinescu, P. J., L. Cucurull, K. Apodaca, L. Bucci, and I. Genkova, 2022: The characterization and impact of Aeolus wind profile observations in NOAA's regional tropical cyclone model (HWRF), **148(749)**, 3491-3508, https://doi.org/10.1002/qj.4370.

Mesinger, F., and Coauthors, 2006: North American Regional Reanalysis. *Bull. Amer. Meteor. Soc*., **87(3)**, 343-360, https://doi.org/10.1175/BAMS-87-3-343.

Morris, M. T., J. R. Carley, E. Colón, A. Gibbs, M. S. F. V. De Pondeca, and S. Levine, 2020: A Quality Assessment of the Real-Time Mesoscale Analysis (RTMA) for Aviation. *Wea. Forecasting*, **35**, 977-996, https://doi.org/10.1175/WAF-D-19-0201.1.

National Academies of Sciences, Engineering, and Medicine, 2016: Next Generation Earth System Prediction: Strategies for Subseasonal to Seasonal Forecasts. Washington, DC: The National Academies Press, 350 pp, https://doi.org/10.17226/21873.

Parrish, D. F., and J. C. Derber, 1992: The National Meteorological Center's Spectral Statistical-Interpolation Analysis System. *Mon. Wea. Rev*., **120(8)**, 1747-1763, https://doi.org/10.1175/1520-0493(1992)120%3C1747:TNMCSS%3E2.0.CO;2.

Poterjoy, J., and F. Zhang, 2016: Comparison of Hybrid Four-Dimensional Data Assimilation Methods with and without the Tangent Linear and Adjoint Models for Predicting the Life Cycle of Hurricane Karl (2010). *Mon. Wea. Rev*., **144**, 1449–1468, https://doi.org/10.1175/MWR-D-15-0116.1.

Purser, R.J., 2018a: Hilbert curves isometrically filling a spherical shell, and their application to the estimation of spatial data density. *NOAA NCEP Office Note*, 49, 23 pp., https://doi.org/10.7289/V5/ON-NCEP-494.

Purser, R. J., 2018b: Convenient Parameterizations of super-logistic probability models of effective observation error. *NOAA NCEP Office Note,* 495, 8 pp., https://doi.org/10.25923/kvmz-vf34.

Rogers, E., T. L. Black, D. G. Deaven, G. J. DiMego, Q. Zhao, M. Baldwin, N. W. Junker, and Y. Lin, Y., 1996: Changes to the Operational "Early" Eta Analysis/Forecast System at the National Centers for Environmental Prediction. *Wea. Forecasting*, **11(3)**, 391-413, https://doi.org/10.1175/1520-0434(1996)011%3C0391:CTTOEA%3E2.0.CO;2.

Rudlosky, S., S. Goodman, K. Calhoun, C. Schultz, A. Back, B. Kuligowski, S. Stevenson, and C. Gravelle, 2020: Geostationary Lightning Mapper Value Assessment. *NOAA Technical Report NESDIS*, **153**, https://doi.org/https://doi.org/10.25923/2616-3v73.

Saha, S., and Coauthors, 2006: The NCEP Climate Forecast System, *Journal of Climate*, **19(15)**, 3483-3517, https://doi.org/10.1175/JCLI3812.1.

Saha, S., and Coauthors, 2010: The NCEP Climate Forecast System Reanalysis. *Bull. Amer. Meteor. Soc.*, **91**, 1015-1058, https://doi.org/10.1175/2010BAMS3001.1.

Shao, H., K. Bathmann, L. Cucurull, R. Treason, D. Kleist, 2023: Initial implementation of COSMIC-2 radio occultation data assimilation for the NCEP Global Operational Forecast System. In preparation.

Shutts, G., 2005: A kinetic energy backscatter algorithm for use in ensemble prediction systems. *Quart. J. Roy. Meteor. Soc.*, **131**, 3079-3102, https://doi.org/10.1256/qj.04.106.

Simmons, A. J., and A. Hollingsworth, A., 2002: Some aspects of the improvement in skill of numerical weather prediction. *Quart. J. Roy. Meteor. Soc.*, **128**, 647-677, https://doi.org/10.1256/003590002321042135.

Tompkins, A. M., and J. Berner, 2008: A stochastic convective approach to account for model uncertainty due to unresolved humidity variability. *J. Geophys. Res.*, **113**, D18101, https://doi.org/10.1029/2007JD009284.

Tong, M., and Coauthors, 2018: Impact of Assimilating Aircraft Reconnaissance Observations on Tropical Cyclone Initialization and Prediction Using Operational HWRF and GSI Ensemble–Variational Hybrid Data Assimilation. *Mon Wea. Rev.*, 146, 4155-4177, https://doi.org/10.1175/MWR-D-17-0380.1.

Trémolet, Y., 2008: Computation of observation sensitivity and observation impact in incremental variational data assimilation. *Tellus A*, **60**, 964-978, https://doi.org/10.1111/j.1600-0870.2008.00349.x.

Unified Forecast System - Steering Committee and Writing Team, 2021: Unified Forecast System (UFS) Strategic Plan: 2021-2025. https://vlab.noaa.gov/documents/12370130/12437941/20210406_UFS_Strategic_Plan_2021-2025_v1.0.pdf/6c42f8c7-9a08-7255-86d1-cb6113e636e8?t=1618491726122.

Wang, X., 2010: Incorporating ensemble covariance in the Gridpoint Statistical Interpolation (GSI) variational minimization: A mathematical framework. *Mon. Wea. Rev.*, **138**, 2990–2995, https://doi.org/10.1175/2010MWR3245.1.

Wang, X., D. Parrish, D. Kleist, and J. Whitaker, 2013: GSI 3DVar-based ensemble–variational hybrid data assimilation for NCEP Global Forecast System: Single-resolution experiments. *Mon. Wea. Rev.*, **141**, 4098–4117, https://doi.org/10.1175/MWR-D-12-00141.1.

Wang, Y., and X. Wang, 2017: Direct Assimilation of Radar Reflectivity without Tangent Linear and Adjoint of the Nonlinear Observation Operator in the GSI-Based EnVar System: Methodology and Experiment with the 8 May 2003 Oklahoma City Tornadic Supercell. *Mon. Wea. Rev.*, **145**, 1447-1471, https://doi.org/10.1175/MWR-D-16-0231.1.

Whitaker, J. S., A. Shlyaeva, S. G. Penny, 2022: A comparison of hybrid-gain versus hybrid-covariance assimilation for global NWP. *J. Adv. Model. Earth Syst.*, **14**, e2022MS003036, https://doi.org/10.1029/2022MS003036.

Whitaker, J. S., and T. M. Hamill, 2012: Evaluating Methods to Account for System Errors in Ensemble Data Assimilation, Mon. Wea. Rev., **140(9)**, 3078-3089, https://doi.org/10.1175/MWR-D-11-00276.1.

Whitaker, J. S., and T. M. Hamill, 2002. Ensemble Data Assimilation without Perturbed Observations, *Mon. Wea Rev.*, **130(7)**, 1913-1924, https://doi.org/10.1175/1520-0493(2002)130%3C1913:EDAWPO%3E2.0.CO;2.

Wilczak, J., and Coauthors, 2015: The Wind Forecast Improvement Project (WFIP): A Public–Private Partnership Addressing Wind Energy Forecast Needs, *Bull. Amer. Meteor. Soc.*, **96(10)**, 1699-1718, https://doi.org/10.1175/BAMS-D-14-00107.1.

Wilson, A. M., and Coauthors, 2022: Atmospheric River Reconnaissance Workshop Promotes Research and Operations Partnership, *Bull. Amer. Meteor. Soc.*, **103(3)**, E810-E816, https://doi.org/10.1175/BAMS-D-21-0259.1.

Wolfe, D. E., and S. I. Gutman, 2000: Developing an Operational, Surface-Based, GPS, Water Vapor Observing System for NOAA: Network Design and Results. *J. Atmos. Oceanic Technol.*, **17**, 426-440, https://doi.org/10.1175/1520-0426(2000)017%3C0426:DAOSBG%3E2.0.CO;2.

Wu, W.-S., R. J. Purser, and D. F. Parrish, 2002: Three-Dimensional Variational Analysis with Spatially Inhomogeneous Covariances. *Mon. Wea. Rev.*, **130(12)**, 2905-2916, https://doi.org/10.1175/1520-0493(2002)130%3C2905:TDVAWS%3E2.0.CO;2.

Wu, W.-S., D. F. Parrish, E. Rogers, and Y. Lin, 2017: Regional ensemble–variational data assimilation using global ensemble forecasts. *Wea. Forecasting*, **32**, 83–96, https://doi.org/10.1175/WAF-D-16-0045.1.

Yang, R., R. J. Purser, J. R. Carley, M. Pondeca, Y. Zhu, and S. Levine, 2020: Application of a Nonlinear Transformation Function to the Variational Analysis of Visibility and Ceiling Height. *NCEP Office Note*, No. 502, 38 pp, https://doi.org/10.25923/esw8-5n84.

Zhang, F., C. Snyder, and J. Sun, 2004: Impacts of initial estimate and observation availability on convective-scale data assimilation with an ensemble Kalman filter. *Mon. Wea. Rev.*, **132**, 1238–1253, https://doi.org/10.1175/1520-0493(2004)132%3C1238:IOIEAO%3E2.0.CO;2.

Zhou, X., and Coauthors, 2022: The Development of the NCEP Global Ensemble Forecast System Version 12, *Wea. Forecasting*, **37(6)**, 1069-1084, https://doi.org/10.1175/WAF-D-21-0112.1.

Zhou, X., Y. Zhu, D. Hou, and D. T. Kleist, 2016: A Comparison of Perturbations from an Ensemble Transform and an Ensemble Kalman Filter for the NCEP Global Ensemble Forecast System, *Wea. Forecasting*, **31(6)**, 2057-2074, https://doi.org/10.1175/WAF-D-16-0109.1.

Zhu, Y., J.C. Derber, R.J. Purser, B.A. Ballish and J. Whiting, 2015: Variational Correction of Aircraft Temperature Bias in the NCEP's GSI Analysis System. *Mon. Wea. Rev.*, **143**, 3774-3803, https://doi.org/10.1175/MWR-D-14-00235.1.

Zhu, Y., E. Liu, R. Mahajan, C. Thomas, D. Groff, P. Van Delst, A. Collard, D. T. Kleist, R. Treadon, and J. C. Derber, 2016: All-sky microwave radiance assimilation in the NCEP's GSI analysis system. *Mon. Wea. Rev.*, **144(12)**, 4709-4735, https://doi.org/10.1175/MWR-D-15-0445.1.

Zhu, Y., G. Gayno, R. J. Purser, X. Su, and R. Yang, 2019: Expansion of the All-Sky Radiance Assimilation to ATMS at NCEP. *Mon. Wea. Rev.*, **147(7)**, 2603-2620, https://doi.org/10.1175/MWR-D-18-0228.1.

Zupanski, D., M. Zupanski, E. Rogers, D. F. Parrish, and G. DiMego, 2002a: Fine-Resolution 4DVAR Data Assimilation for the Great Plains Tornado Outbreak of 3 May 1999. *Wea. Forecasting*, **17**, 506–525, https://doi.org/10.1175/1520-0434(2002)017<0506:FRDAFT>2.0.CO;2.

Zupanski, M, D. Zupanski, D. F. Parrish, E. Rogers, and G. DiMego, 2002: Four-Dimensional Variational Data Assimilation for the Blizzard of 2000. *Mon. Wea. Rev.*, **130**, 1967–1988, https://doi.org/10.1175/1520-0493(2002)130<1967:FDVDAF>2.0.CO;2.

Appendix A: Observation Processing Reengineering and IODA

IODA is the Interface for Observational Data Access. It is the component of JEDI that ingests and processes observational data for use with other JEDI components. It provides the interfaces that bridge the external observation data to the components with JEDI that utilize those data, namely the Object Oriented Prediction System (OOPS) and the Unified Forward Operator (UFO). IODA is called extensively throughout the JEDI system wherever observation-space data is created, read, and written. As illustrated in Figure A1, IODA deals with generic observation information from the data provider (e.g., GTS Network) and those pre-processed by various NWP centers. IODA also serves as an engine to store and share information related to observations generated during the data assimilation process, such as simulated observations (H(x)), the first-guess departures (O-B), analysis-guess departures (O-A), quality control flags, derived variables, bias correction, and any desirable DA results for diagnostics.

The data structure model in IODA is based on the HDF (Hierarchical Data Format) data model and consists of elements that allow the data to be organized in a similar fashion as a file system (e.g., files in a directory, directories in a directory). The IODA data structure model contains three primary classes: Group, Variables, and Attributes. These classes are combined to create a data structure model resembling a file system structure. The IODA group is analogous to a directory where a Group can contain another Group to form a hierarchical structure. More detailed information on the IODA data model can be found in the IODA section of the online JEDI documentation.

The IODA architecture with its subsystems is illustrated in Figure A2. As described above, IODA data (middle layer) is based on the HDF data model and is organized like a computer file system. The top (storage) layer handles the conversion of various data sources and formats to the standard IODA data model. The result of the conversion can be stored either in memory or written to disk (currently supported file formats include HDF5/netCDF4 and ODB). The bottom layer is the client-facing API layer which handles variables related to observational data in terms of their functionalities. The client API layer and the data model provide a consistent, stable interface for the clients of IODA.

Another important aspect related to IODA data handling is to unify the data conventions (e.g., name, unit, data type) in JEDI. The IODA library is called extensively throughout the JEDI applications wherever observation space data is created, read, and written. It handles observations and data used in data assimilation in general. Besides standardizing the IODA data model, It is also necessary to unify data in terms of their names and units common to JEDI users and developers. For the purpose of unifying the IODA convention, a document with a series of tables was created to provide variable and attribute description, unit, data type, dimensions, and standardized names for all observations and data in the JEDI system. More details can be found in JEDI Data Conventions and Convention Tables from the JEDI Documentation.

Incorporating JEDI components into the NCEP operational DA system requires re-engineering our current observation processing procedures to adapt the standardized IODA data model and unified data convention. The objectives of the re-engineering and related considerations are summarized as follows:

- Develop a robust and user-friendly BUFR converter
    - A C++ tool that converts BUFR data to IODA ObsGroup object (e.g., NetCDF or memory) is under development as part of the IODA engines in JEDI.
    - The mapping between BUFR and IODA will retain the original physical meaning and unit of the BUFR mnemonic without variable transform.
    - Generalize the method of retrieving data from BUFR in IODA. The current NCEP BUFR library prevents users from properly accessing BUFR messages encoded in delayed replication without special handling. Therefore a query utility has been developed in C++ in IODA to generalize the process with precision (Figure A3).
    - The converter can handle various BUFR formats: prepBUFR, NCEP BUFR, and WMO BUFR.
- Implement the quality control and variable transform procedures developed in the prepBUFR processing in JEDI UFO, where data filtering occurs (see Figure A4).
    - Quality control procedures (Figure 3) designed to perform at prepBUFR processing for radiosonde (CQCBUFR), Radar wind profiler (PROFCQC), radar-derived winds from Velocity Azimuth Display (CQCVAD), aircraft (PREPACQC), and basic sanity checks for all data types (PREPDATA) are in JEDI UFO.
    - The variable transform is necessary since the original observations can differ from those required by the DA system. For example, the wind observations are often wind speed and direction, whereas the DA system requires eastward and northward wind components for analysis.
- The BUFR converter will be incorporated into IODA as the backend part of the IODA engines so that the JEDI can read and process BUFR directly. Currently, the BUFR converter is a stand-alone tool.

The BUFR converter is at its final stage of development. Most of the data types from BUFR dump and prepBUFR are under extensive testing. Each data type has a reference observation data set from GDAS for verification to ensure that the BUFR converter works correctly.

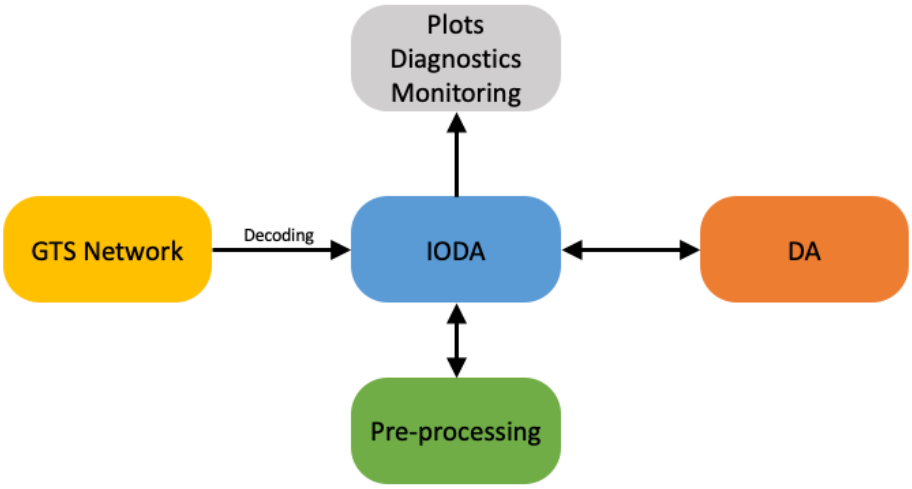

Figure A1. High-level data flow through the IODA subsystem. Figure adapted from online JEDI Documentation.

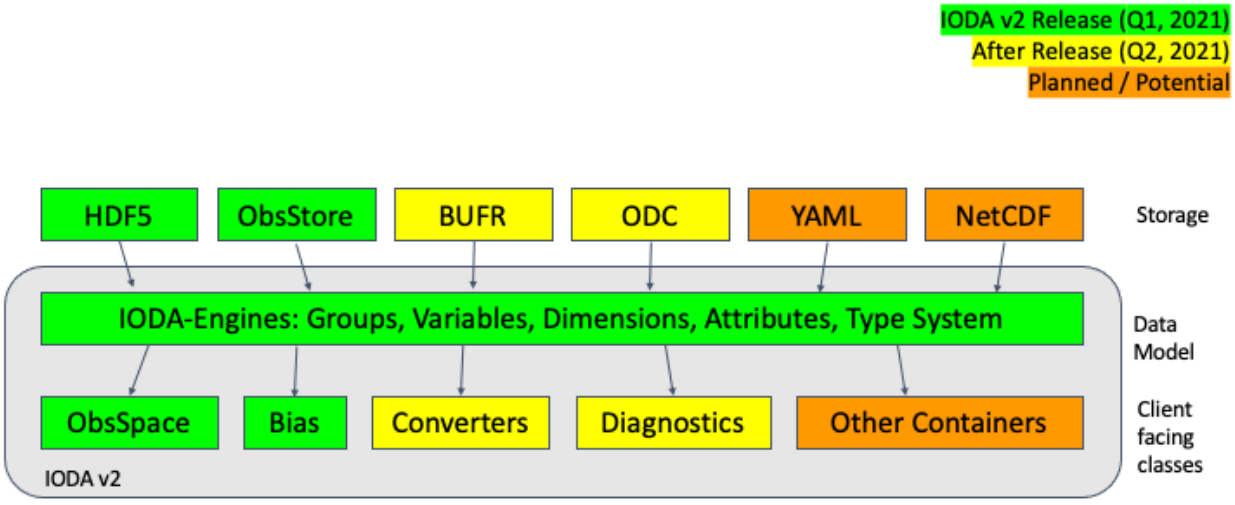

Figure A2. IODA structure and its internal structure of the IODA subsystem.

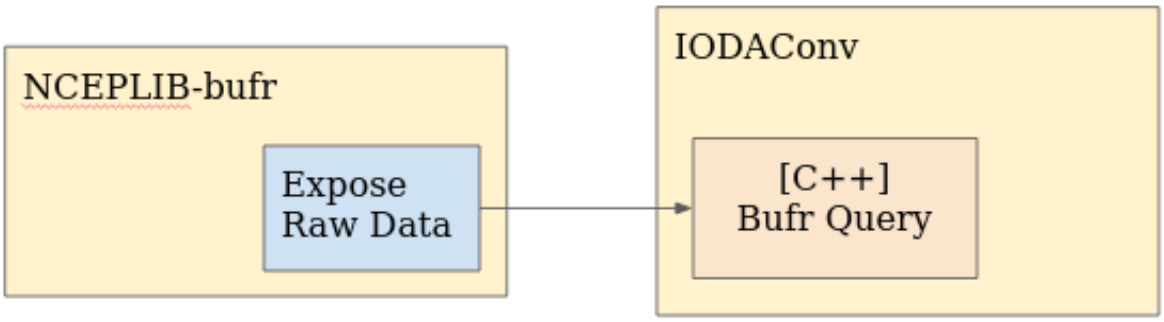

Figure A3. A schematic diagram describing the relationship between the NCEP BUFR library and IODA BUFR converter.

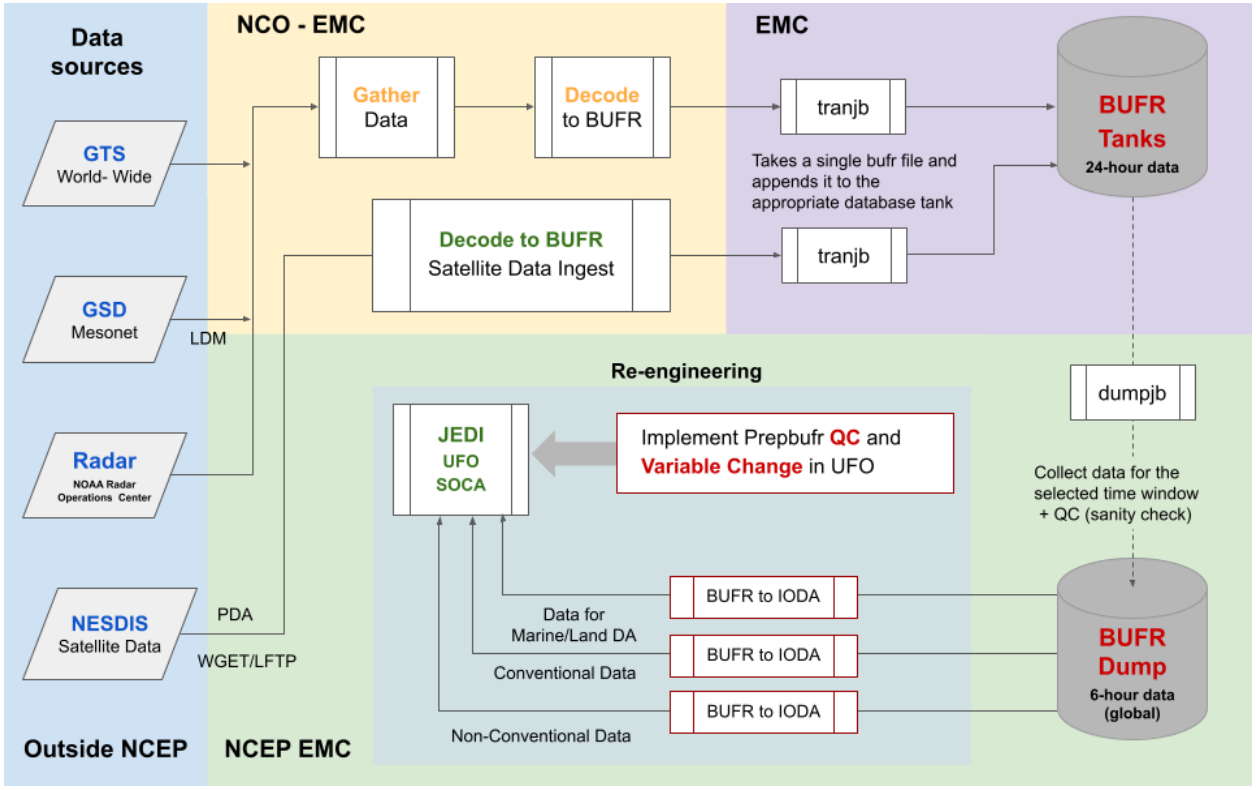

Figure A4. Schematic representation of the revised I ingest, decoding, and observation preprocessing process (the revised part is in the green block).

Appendix B: Abbreviations, Acronyms, and Terminology

2DVar	Two-Dimensional Variational
3DVar	Three-Dimensional Variational
3DEnVar	Three-Dimensional Ensemble Variational
4DVar	Four-Dimensional Variational
4DEnVar	Four-Dimensional Ensemble Variational
ABI	Advanced Baseline Imager
ADA	Advanced Doubling and Adding Method
AHI	Advanced Himawari Imager
AGL	Above Ground Level
AMDAR	Aircraft Meteorological DAta Relay
AMSR	Advanced Microwave Scanning Radiometer
AMSU-A	Advanced Microwave Sounding Unit - A
AMVs	Atmospheric motion vectors
AOD	Aerosol Optical Depth
AoR	Analysis of Record
ASCAT	Advanced Scatterometer
ASCII	American Standard Code for Information Interchange
ASOI	Analysis Sensitivity to Observations Impact
ATMS	Advanced Technology Microwave Sounder
AVHRR	Advanced Very High Resolution Radiometer
BUFR	Binary Universal Form for the Representation of meteorological data
C-MAN	Coastal-Marine Automated Network
CDAS	Climate Data Assimilation System
CFS	Climate Forecast System
CFSR	Climate Forecast System Reanalysis
CICE	Los Alamos sea ice model
CLWP	Cloud liquid water path
COSMIC	Constellation Observing System for Meteorology, Ionosphere and Climate
CPC	Climate Prediction Center
CrIS	Cross-track Infrared Sounder
CRTM	Community Radiative Transfer Model
CSR	Clear sky radiance
CTD	Conductivity Temperature Depth
CW	Cloud water
CWOP	Citizen Weather Observer Program
DA	Data Assimilation
DFI	Digital Filter Initialization
DMSP	Defense Meteorological Satellite Program
DMV(W)s	Derived Motion Vectors (Winds)
DTC	Developmental Testbed Center
ECMWF	European Centre for Medium-Range Weather Forecasts
EFSOI	Ensemble Forecast Sensitivity to Observations Impact
EMC	Environmental Modeling Center

EnKF	Ensemble Kalman Filter
EnSRF	Ensemble Square Root Filter
EOS	Earth Observing System
EUMETSAT	European Organization for the Exploitation of Meteorological Satellites
FSOI	Forecast Sensitivity to Observations Impact
FV3	Finite-Volume Cubed-Sphere dynamical core
GDAS	Global Data Assimilation System
GEFS	Global Ensemble Forecast System
GEOS	Goddard Earth Observing System model
GFDL	Geophysical Fluid Dynamics Laboratory
GFS	Global Forecast System
GLDAS	Global Land Data Assimilation System
GMI	Global Precipitation Measurement Microwave Imager
GNSS	Global Navigation Satellite System
GODAS	Global Ocean Data Assimilation System
GOES	Geostationary Operational Environmental Satellites
GOME	Global Ozone Monitoring Experiment
GPS	Global Positioning System
GSI	Gridpoint Statistical Interpolation analysis system
GTS	Global Telecommunication System
HAFS	Hurricane Analysis and Forecast System
HDF	Hierarchical Data Format
HDOB	High-Density Observations Bulletin
HRRR	High Resolution Rapid Refresh
HWRF	Hurricane Weather Research and Forecasting model
HYCOM	HYbrid Coordinate Ocean Model
IASI	Infrared Atmospheric Sounding Interferometer
IAU	Incremental Analysis Update
IODA	Interface for Observational Data Access
IR	Infrared
JCSDA	Joint Center for Satellite Data Assimilation
JEDI	Joint Effort for Data assimilation Integration
JPSS	Joint Polar Satellite System
LEO	Low Earth Orbit
LETKF	Local Ensemble Transform Kalman Filter
LIDAR	Light Detection and Ranging
LIS	Land Information System
MDCRS	Meteorological Data Collection and Reporting System
METAR	aviation routine weather report
MHS	Microwave Humidity Sounding
MLS	Microwave Limb Sounder
MODIS	Moderate-resolution Imaging Spectro-radiometer
MOM	Modular Ocean Model
MOU	Memorandum of Understanding

MRW	Medium-Range Weather
MW	Microwave
NAM	North American Mesoscale forecast system
NASA	National Aeronautics and Space Administration
NCAR	National Center for Atmospheric Research
NCO	NCEP Central Operations
NCODA	US Navy Coupled Ocean Data Assimilation system
NCEP	National Centers for Environmental Prediction
NDAS	North American Data Assimilation System
NDFD	National Digital Forecast Database
NEMS	NOAA Environmental Modeling System
NESDIS	National Environmental Satellite, Data, and Information Service
NEXRAD	Next Generation Weather Radar
NLDAS	North American Land Data Assimilation System
NOAA	National Oceanic and Atmospheric Administration
NPS	NCEP Production Suite
NSST	Near Sea Surface Temperature
NWP	Numerical Weather Prediction
NWS	National Weather Service
OAR	NOAA Office of Oceanic and Atmospheric Research
ODB	ECMWF Observation DataBase
OMF	Observation Minus Forecast
OMI	Ozone Monitoring Instrument
OMPS	Ozone Mapping and Profiler Suite
OOPS	Object-Oriented Prediction System
OSEs	Observing System Experiments
PDF	Probability Density Function
POES	Polar Operational Environmental Satellites
PWAT	Precipitable water
QC	Quality Control
R2O	Research to Operations
RADAR	Radio Detection and Ranging
RAP	Rapid Refresh
RASS	Radio Acoustic Sounding System
RO	Radio Occultation
RRFS	Rapid Refresh Forecast System
RTMA	Real-Time Mesoscale Analysis
RTOFS	Real-Time Ocean Forecast System
S2S	Subseasonal-to-Seasonal
SBUV	Solar Backscatter Ultraviolet
SDL	Scale-dependent localization
SEVIRI	Spinning Enhanced Visible Infra-Red Imager
SHEF	Standard Hydrologic Exchange Format
SKEB	Stochastic Kinetic Energy Backscatter

SNPP	Suomi National Polar-orbiting Partnership
SPECI	aviation special weather report
SPPT	Stochastically Perturbed Parameterization Tendencies
SSI	Spectral Statistical Interpolation analysis system
SSMIS	Special Sensor Microwave - Imager/Sounder
SST	Sea surface temperature
SYNOP	Surface synoptic observation
TAC	Traditional Alphanumeric Codes
TAMDAR	Tropospheric Airborne Meteorological Data Reporting
TLNMC	Tangent-linear Normal Model Constraint
TROPOMI	TROPOspheric Monitoring Instrument
UCAR	University Corporation for Atmospheric Research
UFO	Unified Forward Operator
UFS	Unified Forecast System
URMA	UnRestricted Mesoscale Analysis
UTC	Universal Coordinated Time
UV	Ultraviolet
VAD	Velocity Azimuth Display
VarBC	Variational Bias Correction
VarQC	Variational Quality Control
VIIRS	Visible/Infrared Imager Radiometer Suite
WDAS	Whole atmosphere Data Assimilation System
WMO	World Meteorological Organization
WRF	Weather Research and Forecasting model
XBTs	eXpendable Bathythermographs